

# Prednisolone reduces the interferon response to AAV in cynomolgus macaques and may increase liver gene expression

Lili Wang,<sup>1</sup> Claude C. Warzecha,<sup>1</sup> Alexander Kistner,<sup>2</sup> Jessica A. Chichester,<sup>1</sup> Peter Bell,<sup>1</sup> Elizabeth L. Buza,<sup>1</sup> Zhenning He,<sup>1</sup> M. Betina Pampena,<sup>3</sup> Julien Couthouis,<sup>2</sup> Sunjay Sethi,<sup>4</sup> Kathleen McKeever,<sup>2</sup> Michael R. Betts,<sup>3</sup> Emil Kakkis,<sup>2</sup> James M. Wilson,<sup>1</sup> Samuel Wadsworth,<sup>5</sup> and Barbara A. Sullivan<sup>2</sup>

<sup>1</sup>Gene Therapy Program, Department of Medicine, Perelman School of Medicine, University of Pennsylvania, Philadelphia, PA 19104, USA; <sup>2</sup>Ultragenyx Pharmaceutical Inc., 60 Leveroni Ct, Novato, CA 94949, USA; <sup>3</sup>Department of Microbiology, Perelman School of Medicine, University of Pennsylvania, Philadelphia, PA 19104, USA; <sup>4</sup>Charles River Laboratories Inc., Reno, NV 89511, USA; <sup>5</sup>Ultragenyx Gene Therapy, Ultragenyx Pharmaceutical Inc., Cambridge, MA 02139, USA

**Ornithine transcarbamylase deficiency is a rare X-linked genetic urea cycle disorder leading to episodes of acute hyperammonemia, adverse cognitive and neurological effects, hospitalizations, and in some cases death. DTX301, a non-replicating, recombinant self-complementary adeno-associated virus vector serotype 8 (scAAV8)-encoding human ornithine transcarbamylase, is a promising gene therapy for ornithine transcarbamylase deficiency; however, the impact of sex and prophylactic immunosuppression on ornithine transcarbamylase gene therapy outcomes is not well characterized. This study sought to describe the impact of sex and immunosuppression in adult, sexually mature female and male cynomolgus macaques through day 140 after DTX301 administration. Four study groups (n = 3/group) were included: male non-immunosuppressed; male immunosuppressed; female non-immunosuppressed; and female immunosuppressed. DTX301 was well tolerated with and without immunosuppression; no notable differences were observed between female and male groups across outcome measures. Prednisolone-treated animals exhibited a trend toward greater vector genome and transgene expression, although the differences were not statistically significant. The hepatic interferon gene signature was significantly decreased in prednisolone-treated animals, and a significant inverse relationship was observed between interferon gene signature levels and hepatic vector DNA and transgene RNA. These observations were not sustained upon immunosuppression withdrawal. Further studies may determine whether the observed effect can be prolonged.**

## INTRODUCTION

Ornithine transcarbamylase (OTC) deficiency is the most common urea cycle disorder, accounting for roughly 50% of inborn errors of urea synthesis, and has an incidence of 1/56,500 newborns in the United States.<sup>1</sup> The OTC gene, located on the short arm of the X chromosome at Xp21.1, is responsible for the conversion of ornithine and carbamoyl phosphate to citrulline in the liver as part of the urea cycle;

a lack of OTC activity leads to the accumulation of ammonium and glutamine, decreased or absent citrulline, and increased urinary orotic acid.<sup>2,3</sup> OTC deficiency can affect both males and females. Males with complete OTC deficiency present with acute, often fatal hyperammonemia in the first week of life, whereas those with partial deficiency have a late presentation, often in adulthood,<sup>3</sup> with the majority of identified female patients experiencing late-onset disease. Consequently, there exists a clinical spectrum of disease severity, the most serious of which include seizures, coma, and death.<sup>3</sup>

Treatment options for OTC deficiency are generally limited to a protein-restricted diet, ammonia scavengers, and liver transplantation.<sup>2,4</sup> Approved therapies (sodium phenylbutyrate, glycerol phenylbutyrate, sodium phenylacetate, and sodium benzoate), which must be taken multiple times per day for the patient's entire life, do not eliminate the risk of future metabolic crises. Currently, the only curative approach is liver transplantation with the accompanying risk of exposure to lifelong immunosuppressive drugs. While liver transplantation will not undo previously acquired neurological damage, it can allow an unrestricted diet and decreased reliance on medication.<sup>4</sup>

Given that OTC deficiency is a monogenic disorder, it is a promising candidate for the development of gene therapy with adeno-associated virus (AAV)-based vectors. DTX301 (avalotcagene ontaparvovec) is an investigational product consisting of a codon-optimized, human, wild-type OTC gene with a liver-specific promoter and enhancer packaged in a self-complementary AAV8 vector. DTX301 is administered as a single peripheral intravenous infusion designed to deliver durable hepatic gene expression and prevent complications associated with OTC deficiency.<sup>5</sup> In preclinical studies, DTX301 normalized levels of urinary orotic acid (a marker of ammonia metabolism),

Received 19 August 2021; accepted 16 January 2022;  
<https://doi.org/10.1016/j.omtm.2022.01.007>

**Correspondence:** Barbara A. Sullivan, PhD, Immunology & Biomarker Strategy, Ultragenyx Pharmaceutical Inc., 81 Digital Drive, Novato, CA 94949, USA.  
**E-mail:** [bsullivan@ultragenyx.com](mailto:bsullivan@ultragenyx.com)



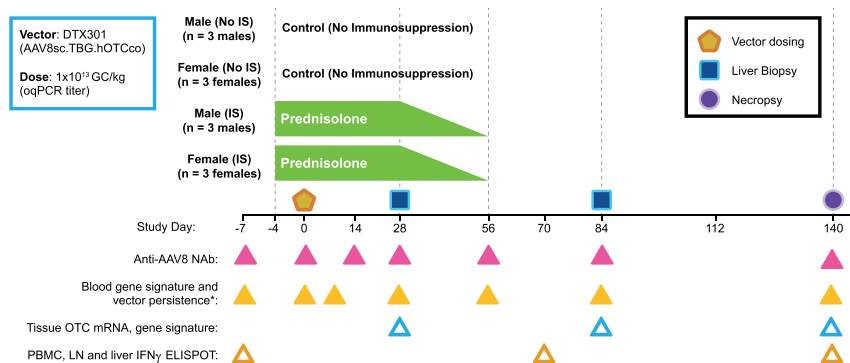


**Figure 1. Study design**

Cynomolgus macaques were administered intravenously (i.v.) with  $1 \times 10^{13}$  genome copies (GCs)/kg of AAV8sc.TBG.hOTCco with no immunosuppression (IS) or prednisolone (1 mg/kg/day). Prednisolone was initiated 4 days prior (day -4) to vector administration and tapered between days 28 and 56 by approximately 25% per week. Two consecutive liver biopsies were performed on all animals on days 28 and 84, respectively. Necropsy and terminal collections were performed on day 140. Anti-AAV8 neutralizing antibodies (NAbs), vector DNA and IFN gene signature in the blood, vector DNA, human codon-optimized OTC (hOTCco) messenger RNA (mRNA), IFN gene signature in the liver, and IFN  $\gamma$  ELISPOT were evaluated in individual macaques at the indicated time points (triangles). \*For the IFN signature in the blood, day 0 samples were collected both pre dose and 6 h post dose. LN, lymph node; oqPCR, optimized quantitative polymerase chain reaction; PBMCs, peripheral blood mononuclear cells.

restored OTC enzyme activity, and allowed animals to survive ammonia challenge.<sup>6</sup> Positive safety and efficacy outcomes with DTX301 in adults with late-onset OTC deficiency in a phase 1/2 study allowed for progression to a pivotal trial for the evaluation of DTX301 as a potential new treatment for OTC deficiency.<sup>5,7</sup>

It is well known that the host immune response to AAV vectors can limit therapeutic use.<sup>8–10</sup> Indeed, the production of type I interferons (IFNs) has been shown to play a role in the amplification of adaptive anti-AAV responses.<sup>9,11,12</sup> Although AAV vector systems confer reduced immunological response as compared with other vector systems, immune suppression may provide benefit in maximizing transduction efficiency.<sup>13</sup> Commonly, treatment with corticosteroids is used in conjunction with AAV gene therapy, either prophylactically or reactively, to mitigate immune responses.<sup>14–16</sup> In mice, several studies have demonstrated that hepatocyte transduction efficiency differs between males and females.<sup>17–21</sup> This is of particular interest when studying DTX301, because although OTC deficiency is X-linked and predominantly affects males, approximately 20% of heterozygous females are also symptomatic<sup>22</sup>; therefore, it is important to establish that potential treatment methodologies are effective in both sexes.

The impact of prophylactic immunosuppression (IS) and sex is not well characterized in non-human primate (NHP) models as a surrogate for human response. Further testing in NHPs provides an opportunity to elucidate the potential impact of prophylactic IS and investigate other mechanistic factors that may impact DTX301 efficacy. In the present study, we sought to characterize the impacts of prophylactic IS and sex on the transduction and transgene expression of DTX301 in NHPs to establish safety and efficacy profiles.

## RESULTS

### Study design

A single  $1 \times 10^{13}$  genome copies (GCs)/kg dose of DTX301 was administered to 12 adult, sexually mature female and male cynomolgus macaques, with or without prophylactic IS. Four study groups

(n = 3 per group) were examined: male non-IS; male IS; female non-IS; and female IS. In the IS groups, prednisolone (1 mg/kg/day) was administered 4 days before and for 28 days following DTX301 administration and was tapered approximately 25% per week from days 28 to 56 (Figure 1). In-life liver biopsies were collected on day 28 and day 84, and terminal liver samples were scheduled for assessment on day 140.

### Baseline animal characteristics

Age at DTX301 dosing ranged from 4.8 to 12.8 years, and weight at dosing ranged from 3.4 to 12.8 kg (Table 1). Male and female animals were randomly assigned to the non-IS or IS groups and were not age or weight matched across study groups. Mean female age at baseline was approximately 2 years older than mean age at baseline for male animals; however, the difference was not statistically significant, and age was evenly distributed within the two groups of female animals (Figure S1). Of note, 1 male aged 4.8 years may have been on the cusp of sexual maturity and was not absolutely confirmed as sexually mature.<sup>23</sup>

### Longitudinal animal characteristics

Individual animal body weights were generally stable throughout the course of the study. DTX301 was generally well tolerated by all animals, with only one animal (BQ652) requiring an unscheduled necropsy at day 103 due to iatrogenic surgical site dehiscence 19 days after the second liver biopsy procedure that was considered unrelated to DTX301 or prednisolone treatment.

Alanine aminotransferase (ALT) and aspartate aminotransferase (AST) were examined over the course of the study to assess overall liver health following DTX301 administration (Figure S2). Mean baseline values for ALT were slightly higher in females than males, although this difference did not reach significance. During the course of the study, ALT levels increased to at least double that of mean pre-dosing levels (baseline) in the majority (9/12) of the study animals, including all six animals in the non-IS groups and three animals in

**Table 1. Baseline animal age and weight**

Group	Sex	Immunosuppression	ID	Age at dosing (y)	Weight (kg)
M (no IS)	M	none	BB927D	8.4	12.78
			CEA029	4.8	4.94
			T3800	12.6	5.72
F (no IS)	F	none	BC829	12.8	4.38
			BG126	12.3	5.04
			BA531K	8.5	3.70
M (IS)	M	prednisolone	BA990K	6.6	6.10
			BB436F	8.9	8.95
			CCC050	6.7	6.76
F (IS)	F	prednisolone	BG407	12.5	5.80
			BQ652 <sup>a</sup>	10.7	4.96
			CCG015	6.3	3.40

F, female; IS, immunosuppression; M, male.  
<sup>a</sup>BQ652 (group 4) was euthanized on day 103 due to complications from the incision after the day 84 liver biopsy.

the IS groups (Figures S2A and S2B). For the three animals in the IS groups, ALT elevations mostly occurred on or after day 56, when IS was withdrawn, whereas the elevations observed in animals in the non-IS groups did not show a clear association with a particular time point. Four animals showed ALT elevations as early as day 7 after dosing: three in the non-IS group and one in the female IS group. AST levels were generally low throughout the study; any increases were not associated with particular groups or time points. ALT and AST levels resolved without intervention and remained within reported reference ranges for male and female cynomolgus macaques.<sup>24</sup>

In order to characterize the levels of vector persistence in the blood over the course of the study, blood samples were analyzed for vector DNA content. Vector in blood had two phases of reduction: early (within the first week) and late (approximately 20 weeks; Figure S3A). Across all groups, the levels of vector DNA detected in blood at 6 h post DTX301 administration was approximately three logs higher than on day 7; residual vector DNA in the blood decreased gradually toward the end of the study. Overall levels of vector in whole blood (GCs/mL) were similar between groups across all time points (Figure S3A).

Mean vector DNA levels in peripheral blood mononuclear cells (PBMCs) were assessed for all groups on study days 70 and 140 to compare with the whole blood measurements (Figure S3B). Mean vector DNA levels in PBMCs at day 70 and day 140 were similar, in contrast with the sharp decrease observed in whole blood from day 70 to day 140, coincident with turnover of RBCs. These findings are consistent with previously published studies in a hemophilia A trial with an AAV5 vector, despite the difference in AAV serotype.<sup>25</sup>

All animals developed a positive response in the anti-AAV8 neutralizing antibody (NAb) assay by day 14, which persisted through nec-

ropsy at day 140 (Figure S4). No notable trends were observed in any study group with regard to the kinetics or magnitude of the response.

### Transduction efficiency in the liver

The kinetics and levels of transduction in liver were evaluated by vector GC and human codon-optimized OTC (hOTCco) messenger RNA (mRNA) levels in consecutive liver biopsies at day 28 and day 84 and post necropsy on day 140 (Figure 2). One animal, BQ652, was euthanized on day 103 due to iatrogenic surgical site dehiscence 19 days after the second liver biopsy procedure. Vector GC and hOTCco mRNA levels both were highest at day 28 and significantly reduced at day 84 in all animals, while the overall changes between day 84 and day 140 were not statistically significant (Figure 2A). On average, IS animals exhibited greater vector genome and transgene expression compared with non-IS animals at day 28, although the differences are not statistically significant (Figures 2B and 2C). By day 84 and day 140, similar levels of vector GC and transgene expression were detected in the two groups (IS versus non-IS). No notable differences were observed between male and female IS or non-IS groups at any time point with regard to vector genome and transgene expression (Figures 2B and 2C). On average, vector GCs in liver on day 84 were reduced to  $45.2\% \pm 3.5\%$  (mean  $\pm$  standard error of the mean [SEM];  $n = 12$ ) of those on day 28, and hOTCco mRNA on day 84 were  $41.2\% \pm 4.7\%$  of those on day 28 (Figures S5A and S5B). Vector GCs and hOTCco mRNA on day 140 were at similar levels to those on day 84 ( $94.5\% \pm 7.9\%$  and  $94.2\% \pm 7.2\%$ , respectively).

### Analysis of transgene expression

For analysis of transgene expression, *in situ* hybridization (ISH) (Figure 3) and immunohistochemistry (IHC; Figure 4) were performed. ISH was performed with a probe specific for hOTCco, whereas an antibody against human OTC was used for immunostaining that also detected to some degree endogenous NHP OTC. Both ISH and IHC showed transgene expression predominantly in hepatocytes near portal regions, mimicking to a certain degree the natural distribution of OTC expression (Figures S6 and S7).

A trend was observed toward a greater proportion of positive hOTCco hybridization signal in the cytoplasm of IS animals compared with non-IS animals, as measured by visual inspection (Figure 3A); however, image analysis of proportion of hOTCco-positive cytoplasm and/or nuclei showed no apparent differences between IS and non-IS animals (Figures 3C–3E). The mean  $\pm$  SEM hOTCco expression was approximately  $60\% \pm 5.1\%$  at day 28 and reduced to approximately  $33\% \pm 3.8\%$  and  $16\% \pm 1.8\%$  at day 84 and day 140, respectively (Figure 3B). Similar results were observed for image analysis of proportion of hOTCco hybridization signal in the cytoplasm (Figure S8); however, IS animals trended to show greater hOTCco expression compared with non-IS animals at day 28 (Figure S8B).

OTC protein expression assessed by IHC staining was higher in all DTX301-treated animals by visual inspection, as compared with

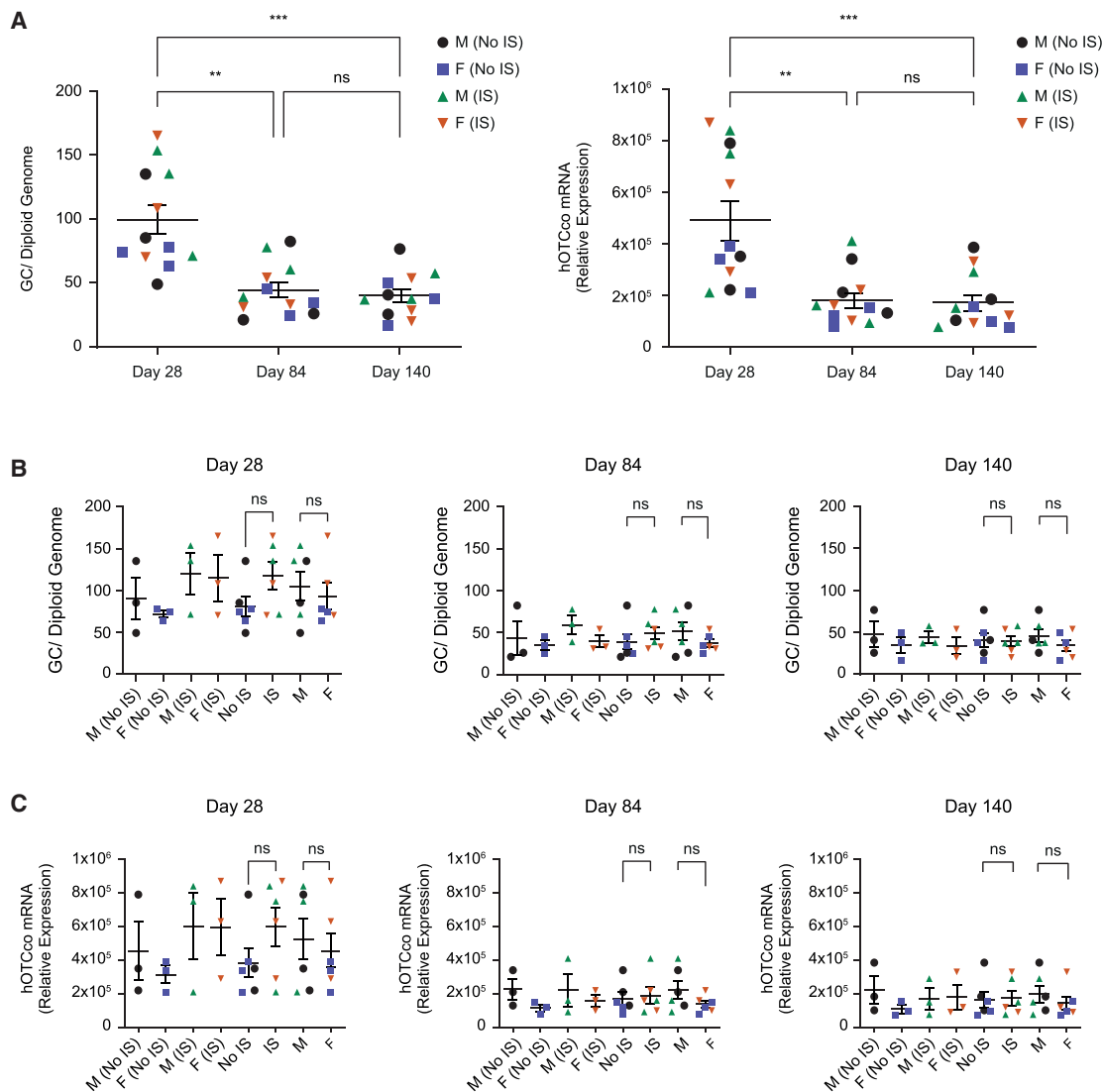


**Figure 2. Vector DNA and hOTCco mRNA analysis**

Vector DNA and hOTCco mRNA were quantified in liver biopsies of individual cynomolgus macaques at day 28, day 84, and day 140. Vector DNA was measured by quantitative polymerase chain reaction (qPCR) and hOTCco mRNA by real-time qPCR. Vector DNA and hOTCco mRNA levels are shown by (A) day and (B and C) individual group. Data are represented as individual values for each animal with mean  $\pm$  SEM. Statistical analysis was performed using a Friedman test with Dunn's multiple comparisons test for (A) and a Mann-Whitney test for (B and C). ns, not significant; \*\* $p = 0.0033$ ; \*\*\* $p = 0.0001$ . F, female; GCs, genome copies; IS, immunosuppression; M, male. See also [Figure S5](#).

untreated NHPs and an OTC-null patient control; this was evident on day 28 and decreased on days 84 and 140 ([Figures 4A and S7](#)). Image analysis was used to estimate the proportion of OTC-positive area ([Figures 4B–4E](#)). The mean  $\pm$  SEM OTC-positive area was approximately  $40\% \pm 1.5\%$  at day 28 and was reduced to approximately  $21\% \pm 2.4\%$  and  $18\% \pm 1.4\%$  at day 84 and day 140, respectively ([Figure 4B](#)). At day 84, a trend was observed for increased OTC-positive area in IS animals compared with non-IS animals ([Figure 4D](#)). Overall, the ISH and IHC data corroborated the trend observed in vector GC and mRNA levels.

#### Exploratory analysis of interferon gene signature

Animals without IS treatment showed an immune response to DTX301 characterized by a rise in the hepatic IFN gene signature on day 28, as compared with animals with IS and control tissues ([Figure 5](#)). Inter-lobe concordance was observed between control samples ([Figure S9](#)). At day 28, the hepatic IFN gene signature was significantly reduced in IS animals compared with the non-IS group (mean  $\pm$  SEM,  $0.11 \pm 0.02$  versus  $0.27 \pm 0.03$ ;  $p = 0.0023$ ; [Figure 5B](#)). Hepatic IFN gene signature heatmaps with all 21 genes showed the effect of prednisolone through independent clustering in IS and

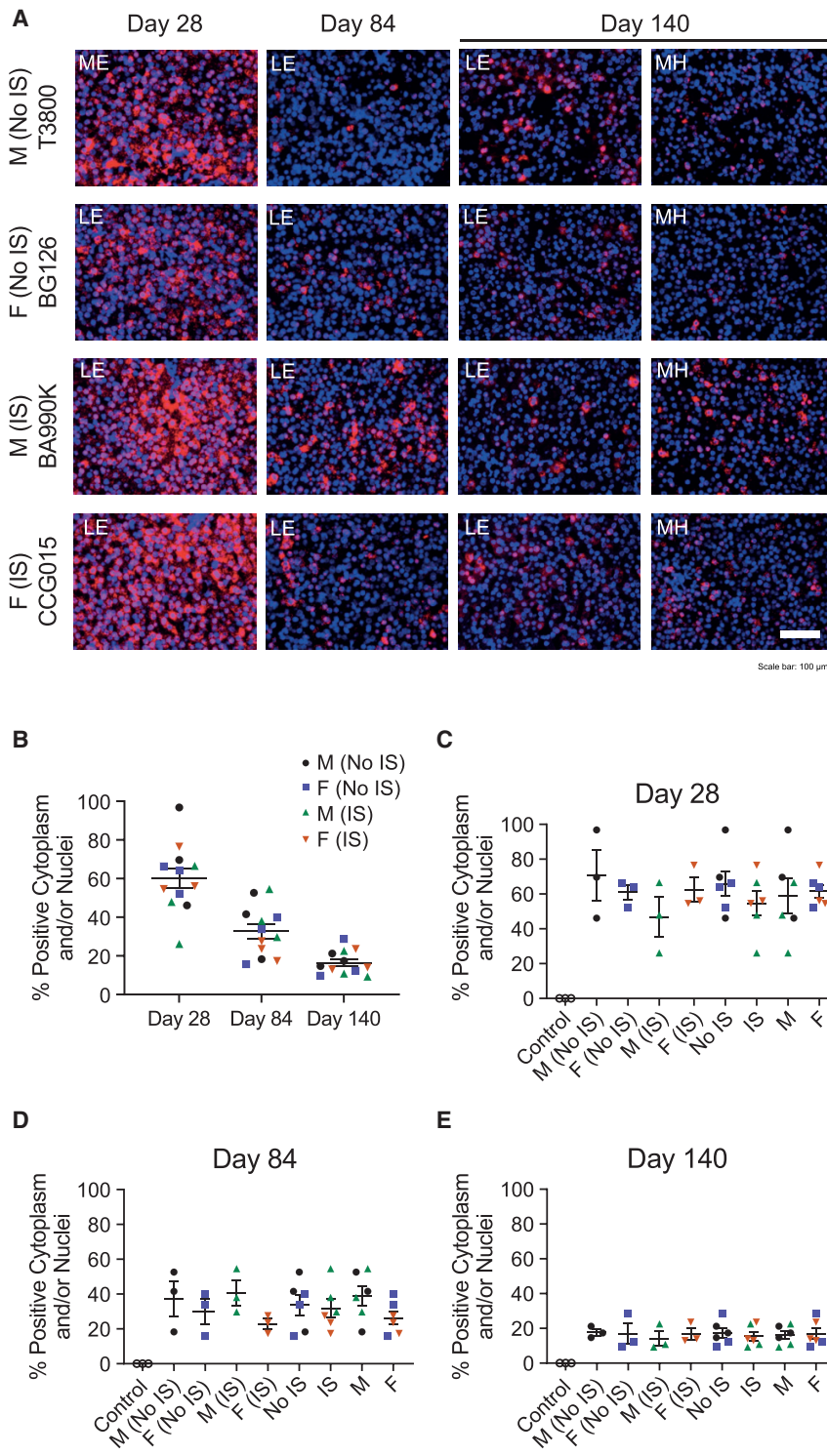


**Figure 3. hOTCco expression in the liver at different time points by *in situ* hybridization**

Transgene expression by hepatocytes was analyzed in liver sections of individual cynomolgus macaques by performing *in situ* hybridization (ISH) at day 28, day 84, and day 140. (A) Representative ISH images (20 $\times$ ) are shown for one animal from each group. Scale bar indicates 100  $\mu$ m. (B–E) hOTCco expression was analyzed using morphology analysis software. Proportion of hepatocytes with positive cytoplasm and/or nuclei is shown by day (B) and for individual groups (C–E). For day 28 and day 84, data are represented as individual biopsy values for each animal with mean  $\pm$  SEM. For day 140, data are represented as the mean of values from two lobes from each animal with mean  $\pm$  SEM. LE, left edge; ME, medial edge; MH, medial hilus. See also Figures S6 and S8.

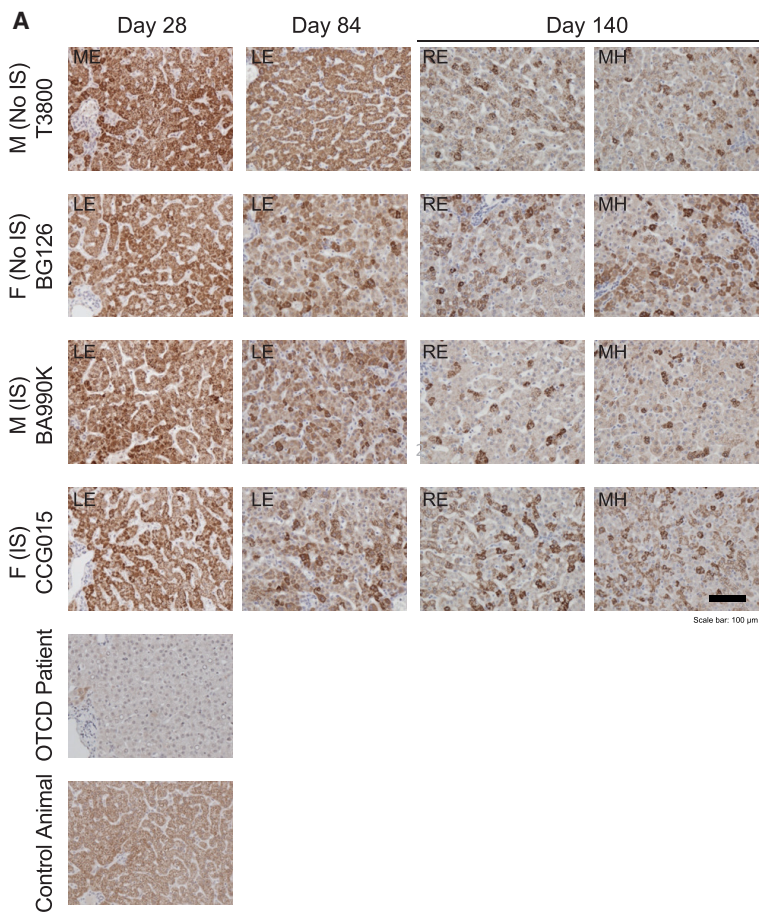
with transduction efficiency. A significant, inverse relationship was observed between levels of hepatic vector DNA and transgene RNA with the IFN gene signature levels at day 28 (Figure 6A). After prednisolone tapering, there was no longer a relationship between IFN gene signature and vector DNA or hOTCco mRNA (Figures 6B and 6C).

To investigate whether the difference in IFN gene signature levels associated with prednisolone was due to altered transcription or cell trafficking, liver composition was examined. Overall, similar levels of mononuclear cell infiltration were observed in the livers of male and female and IS and non-IS animals on day 28 (while IS groups were still receiving prednisolone) as well as day 84 and at necropsy (Table S1). No DTX301-related gross findings were detected from liver biopsy at day 28 or day 84 or at necropsy at day 140. Microscopic findings showed no clear effect of transient IS. There were no observable differences between male and female groups.

Microscopic findings in the liver included hepatocellular cytoplasmic glycogen and/or lipid accumulation, mononuclear cell infiltrates (present in all groups), capsular and subcapsular fibrosis, rare individual hepatocellular necrosis, and hepatocellular multinucleation in some samples. Importantly, these findings have all been reported as background in cynomolgus macaques.<sup>26</sup>

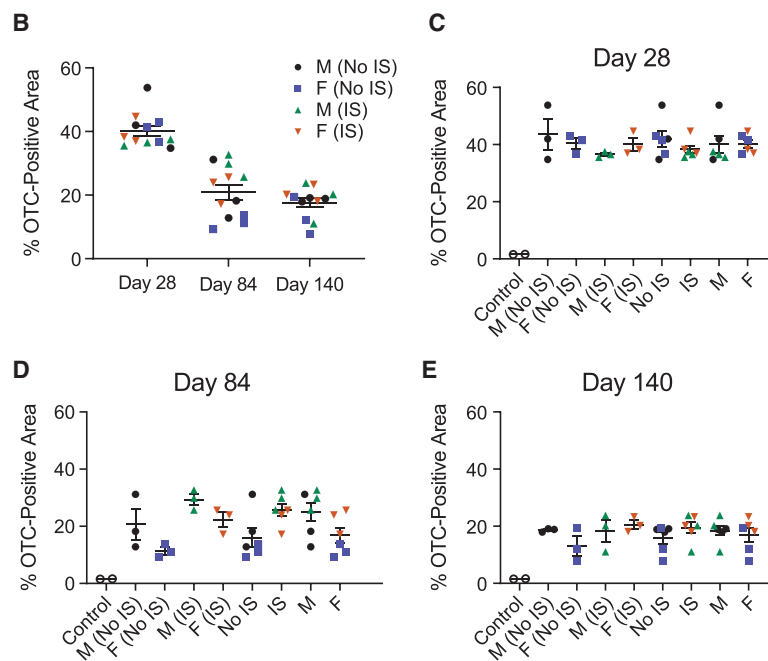
non-IS groups on day 28 (while still receiving prednisolone). Clustering was evident but less clearly defined at later time points (day 84 and day 140) following prednisolone taper (Figures 5A and 5C). We investigated whether hepatocyte IFN gene signatures correlated

The blood IFN gene signature was also evaluated (Figure S10A). Prior to dosing, on day  $-7$ , the females had a significantly elevated blood IFN gene signature compared with the males (female mean 1.06 versus male mean 0.35;  $p = 0.0265$ ), with four of six animals



**Figure 4. hOTC expression in the liver at different time points by immunohistochemistry**

hOTC transgene expression by hepatocytes was analyzed in liver sections of individual cynomolgus macaques by performing immunohistochemistry (IHC) at day 28, day 84, and day 140. (A) Representative IHC images (20 $\times$ ) are shown for one animal from each group. Non-study control and OTCD patient control samples are also shown. Scale bar indicates 100  $\mu$ m. (B–E) hOTC expression was analyzed using Visiopharm software. Proportion of OTC-positive area is shown by day (B) and for individual groups (C–E). For day 28 and day 84, data are represented as individual values for each animal with mean  $\pm$  SEM. For day 140, data are represented as the mean of values from four lobes from each animal with mean  $\pm$  SEM. OTCD, ornithine transcarbamylase deficiency; RE, right edge. See also [Figure S7](#).



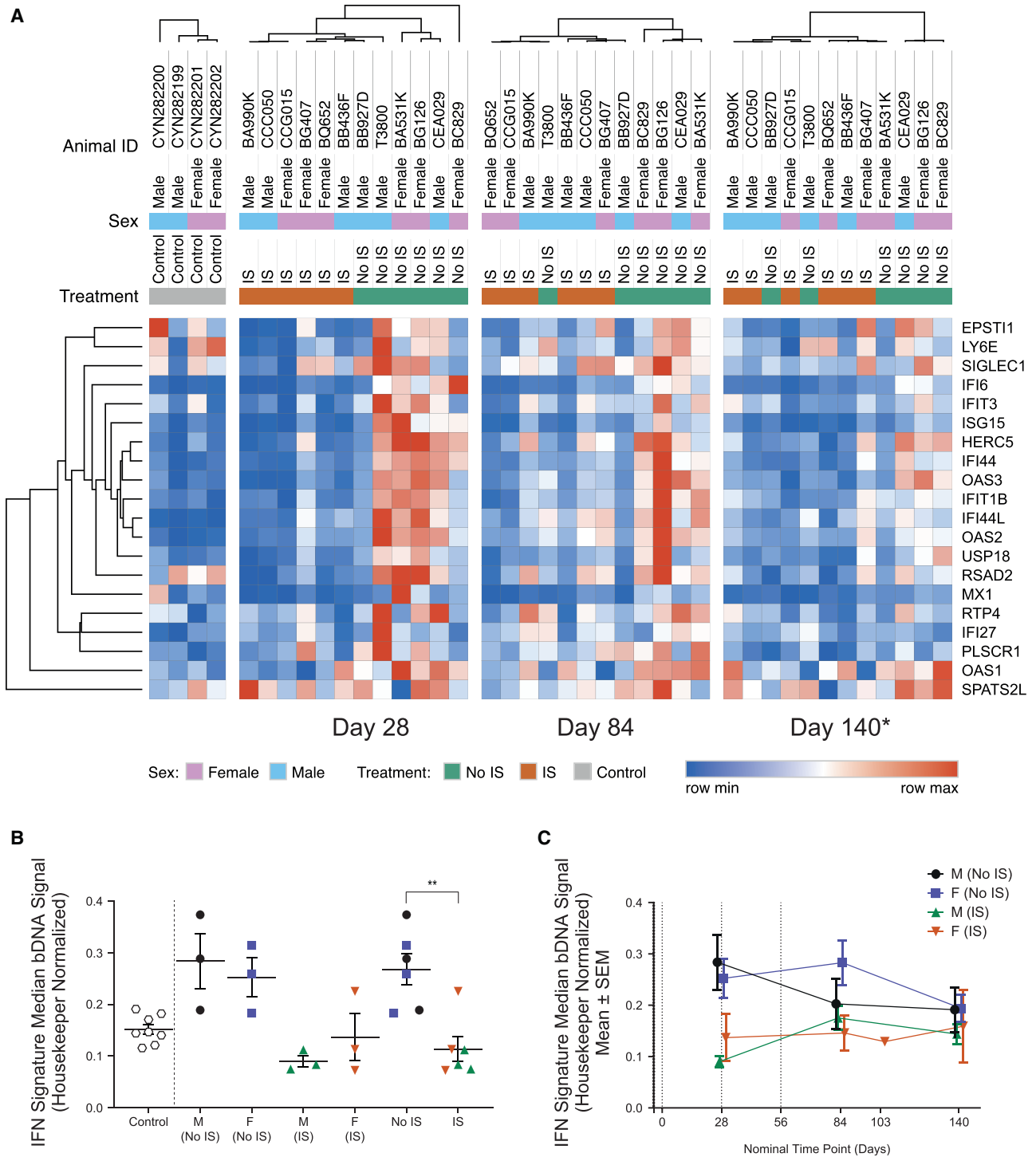


**Figure 5. Analysis of hepatic IFN signature**

The hepatic IFN gene signature was evaluated in individual cynomolgus macaques by determining the expression of 21 IFN-driven genes in liver lysates using a branched (b)DNA assay. (A) Hepatic IFN gene signature heatmaps show all 21 genes at day 28, day 84, and day 140. (B) Hepatic IFN gene signature by group at day 28 for the study animals alongside non-study control liver samples is shown. Data are represented as mean  $\pm$  SEM of the median IFN signature bDNA signal normalized to expression of housekeeping for each animal. (C) Hepatic IFN gene signature at the indicated time points is shown. Data are represented as mean  $\pm$  SEM of the median IFN signature bDNA signal for each group. Statistical analysis was performed using an unpaired t test. \*\* $p = 0.0023$ . \*Animal BQ652 evaluated at day 103. See also [Figure S9](#).

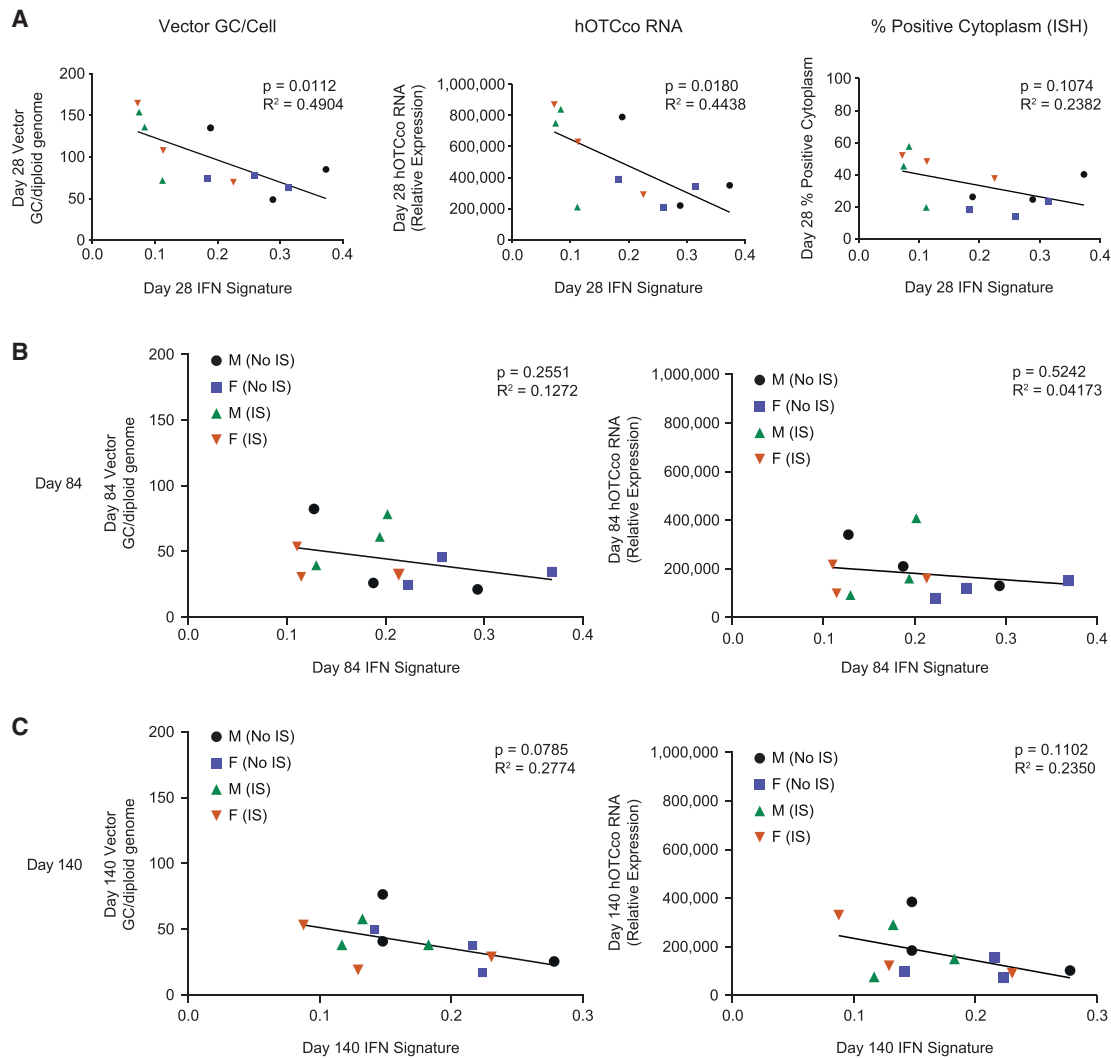


**Figure 6. Correlation analysis of hepatic IFN gene signature**

(A) The hepatic IFN gene signature of individual macaques at day 28 was plotted against vector DNA (left), hOTCco mRNA (middle), and proportion of cytoplasm positive for transgene expression by ISH (right). (B and C) The hepatic IFN gene signature of individual macaques at day 84 (B) and day 140 (C) was plotted against vector DNA (left) and hOTCco mRNA (right). Statistical analysis was performed using a simple linear regression. ISH, *in situ* hybridization.

showing elevated levels compared with control, non-study animals (mean 0.4). At 6 h following gene therapy, the female non-IS group had a significantly higher blood IFN gene signature level compared with the female IS group (female non-IS mean 3.35 versus female IS mean 0.51;  $p = 0.0358$ ). The female with elevated levels prior to prednisolone had control or normal levels following prednisolone and prior to gene therapy on day 0 and then increased upon prednisolone withdrawal. Males had low blood IFN gene signature levels that remained generally stable throughout the study (Figure S10C). Although two female animals with high baseline (day 0) IFN signature in the blood exhibited lower liver vector GCs/cell and hOTCco mRNA expression at day 28 (Figure S11), overall, there was not a significant relationship.

#### IFN $\gamma$ cellular immune response

The cellular immune response to the AAV8 capsid and human OTC (hOTC) protein was analyzed by IFN  $\gamma$  enzyme-linked immunosorbent spot (ELISpot) using corresponding peptide libraries (Figure S12). PBMCs collected at baseline, day 70, and day 140 were evaluated in addition to lymphocytes isolated on day 140 from hilar, axillary, and popliteal lymph nodes as well as the liver.

Overall, there were no notable differences between groups. On day 140, most animals (9/12) had a positive IFN  $\gamma$  response to the AAV8 capsid, specifically peptide pool AAV8-C in liver lymphocytes, with six of these nine animals also demonstrating significant AAV8-C responses in PBMC populations at some point during the study yet



lower in magnitude compared with the response in the liver. The IFN  $\gamma$  response in the lymph nodes remained at baseline levels, with the exception of one animal with a positive hilar lymph node response. Responses to the transgene were far less prominent, with only two animals showing positive responses limited to liver lymphocytes only and characterized as low to moderate in magnitude. There was no apparent correlation between IFN  $\gamma$  ELISpot results and transduction efficiency, as measured by vector GCs and hOTCco mRNA.

To further assess these responses, flow cytometry was performed on lymphocytes isolated from the liver and blood of four animals with elevated ELISpot counts (Figure S13). In the liver, expression of IFN  $\gamma$  and CD107a in CD8<sup>+</sup> T cells was observed in two animals in response to AAV8-C stimulation; however, no IFN  $\gamma$ - or CD107a-expressing CD4<sup>+</sup> T cells were found in blood or liver (Figures S13B–S13D). Minimal expression of other cytokines, such as tumor necrosis factor alpha (TNF- $\alpha$ ) and interleukin-2 (IL-2) was observed within liver CD107 + IFN $\gamma$  + CD8<sup>+</sup> T cells (data not shown). For these measurements, as well as for total B cells, total CD4<sup>+</sup> T cells, total CD8<sup>+</sup> T cells, and CD4<sup>+</sup> T regulatory cells, there were no apparent differences between IS and non-IS animals.

## DISCUSSION

The use of AAV vectors for *in vivo* gene transfer is extremely promising for treating genetic diseases, primarily due to the lack of pathogenicity, the ability to establish long-term transgene expression, and the wide range of possible tissue targets.<sup>27</sup> Given the monogenic origin of OTC deficiency, it is an excellent candidate for treatment by gene therapy. In a phase 1/2 study, six patients, including all three treated at the highest dose, demonstrated a clinically and metabolically stable response.<sup>7</sup> Further, DTX301 was well tolerated, with no serious adverse events, hospitalizations, or other events related to OTC deficiency.<sup>7</sup>

However, certain aspects of gene therapy for OTC deficiency are not well characterized, including the impact of prophylactic IS and sex differences. Therefore, the present analysis sought to characterize the investigational therapy DTX301 in male and female NHPs, with and without prophylactic IS, to inform the development of a safe and effective treatment regimen for patients with OTC deficiency. Broadly, all 12 animals responded to gene therapy and produced hOTCco mRNA and protein. Further, DTX301 was generally well tolerated by all animals. One animal required an unscheduled necropsy at day 103 due to iatrogenic surgical-site dehiscence 19 days post-operative of the day 84 liver biopsy.

IS via corticosteroids (e.g., prednisolone) is a common tactic used to mitigate the immune response to gene therapy and thereby prevent loss of vector transduction.<sup>16</sup> The work presented here included study groups who received IS via prednisolone from 4 days prior to DTX301 administration through day 28 post treatment, followed by an additional 28-day tapering period. These animals were compared with those that did not receive prednisolone in order to characterize the impact of IS on DTX301 transduction efficiency and transgene

expression. Overall, IS appeared to have no considerable effect on blood biodistribution, with vector DNA levels in blood samples similar between IS and non-IS groups across time points assessed. In addition, all animals developed elevated NAb levels as early as day 14 following DTX301 administration, with no observable trend favoring the IS versus non-IS groups. These NAb findings were consistent with other studies of AAV vector-based gene therapies, in which all participants developed capsid-specific antibodies, regardless of whether they received prednisolone.<sup>28</sup>

At the earliest time point at which liver biopsies were performed (day 28), IS animals showed a trend of higher levels of vector DNA and hOTCco mRNA in hepatic tissue when compared with non-IS animals, although the differences were not statistically different. These differences waned by subsequent time points following the prednisolone taper (day 84 and day 140), where both IS and non-IS groups showed similar transgene expression. Of note, in a study of an AAV5 vector-based gene therapy for the treatment of hemophilia A, IS via prednisolone proximal to gene therapy administration resulted in similar increases in target gene (FVIII) expression in humans as in NHPs in the present study.<sup>28</sup> Further, a follow-up study in mice demonstrated that there exists no direct regulation of FVIII gene expression by prednisolone, suggesting that the increased transgene expression is likely due to increased retention of AAV vector genomes.<sup>15</sup>

For gene therapy to treat genetic diseases, such as OTC deficiency, sustained transgene expression and long-term therapeutic effects are desirable. In the present study, we characterized the transduction efficiency and kinetics of hOTC expression in macaque liver at three time points (days 28, 84, and 140) from two consecutive liver biopsy samples and necropsy liver tissues. Vector GC and hOTCco expression in liver measured by quantitative polymerase chain reaction (qPCR) peaked at day 28, significantly reduced to an average of 45% of the peak levels on day 84, and then generally stabilized to the end of the study (day 140). The 2-fold reduction observed in this study was much lower compared with the significant loss of vector GC (one to two logs) and transgene expression levels (two to three logs) in the second biopsies in some of our previous AAV gene-transfer studies performed in NHP using foreign transgenes, such as meganucleases.<sup>29</sup>

It is hypothesized that high CpG content of the codon-optimized transgene may trigger toll-like receptor signaling in tissue-resident immune cells, such as Kupffer cells, to produce type I IFN.<sup>30,31</sup> It is also possible that the cyclic guanosine monophosphate-adenosine monophosphate synthase (cGAS)-stimulator of IFN genes (STING) pathway (sensing cytosolic DNA) or MAVS/MDA-5/RIG-I (sensing double-stranded RNA) in hepatocytes may lead to type I IFN production. Early type I IFN responses lead to activation of the innate and adaptive immune system.<sup>32</sup> Here, we speculate that AAV-transduced hepatocytes produce type I IFN, which signals nearby cells to prepare antiviral mechanisms or adopt an “anti-viral state.”<sup>10</sup> Of note, it is presumed that the IFN signature is produced by leukocytes, as the gene list was curated from stimulation of blood and analysis of

systemic lupus erythematosus blood.<sup>33</sup> In the present study, IS animals showed a reduction in IFN signature compared with non-IS animals, corresponding with greater transgene expression. Therefore, it is our hypothesis that prednisolone acts to prevent expression of IFN-driven genes within leukocytes, thereby preventing leukocyte-mediated killing of AAV-positive hepatocytes and allowing the observed increase in vector GC and diploid cell and hOTCco RNA. Ultimately, prednisolone treatment may preserve vector-expressing cells. In the present study, differences in vector GC and diploid cell and hOTCco RNA between IS and non-IS groups waned with IS tapering through day 56, suggesting that prolonged prednisolone immunosuppression may facilitate greater long-term vector gene expression.

In patients with OTC deficiency, steroids can increase catabolism, thereby raising ammonia levels and increasing the risk of adverse events.<sup>34–38</sup> In an ongoing phase 1/2 study of DTX301, this potential concern was raised early in the program and both reactive and prophylactic corticosteroid regimens were explored; the data collected thus far indicate that prophylactic steroids can be used safely in patients with late-onset OTC deficiency who are metabolically stable and free from intercurrent illness.<sup>7</sup>

Several studies have demonstrated distinct sex differences in the success of AAV-mediated gene therapy in the livers of mice, with females showing reduced transduction efficiency compared with males.<sup>18,20,21</sup> Given the established negative impact of the immune response on gene therapy transduction, coupled with the fact that females typically have a stronger immune response compared with males,<sup>39</sup> it would be reasonable to hypothesize that females might exhibit a stronger immune response than males and therefore demonstrate reduced efficiency following gene therapy administration. However, in the present study, no notable differences between males and females were demonstrated with regard to response to DTX301 administration in NHPs. Indeed, all outcome measures were comparable, including ALT elevation, vector uptake, NAb production, transgene DNA and mRNA production in the liver, and histology analyses. The lack of apparent difference observed in this study is similar to that of previous NHP publications of AAV-mediated gene therapy<sup>40,41</sup> and is a promising finding because it suggests that DTX301 may have comparable efficiency in both females and males with OTC deficiency.

As with any study, there are a number of limitations to consider when appraising the results. Firstly, the investigations were performed in a limited sample size. In addition, the animals were not age or weight matched between treatment groups, because this would have proven difficult due to the use of AAV8-naïve and sexually mature animals. The use of in-life liver biopsies ensured data from the same individual animals across the time frame of the study but may not be representative of the liver as a whole. Furthermore, one animal had an unscheduled necropsy on day 103, further limiting sample size in the female IS group for day 140 outcomes.

In summary, all animals treated with the AAV8-based investigational OTC-deficiency therapeutic DTX301 responded with the production

of hOTCco. There were no notable differences in the efficacy of DTX301 in NHPs attributed to sex. However, animals that underwent prophylactic IS via prednisolone demonstrated a transient increase in transgenic efficiency that waned once IS was tapered. It is hypothesized that prednisolone reduced IFN signaling in infiltrating leukocytes, allowing increased transduction efficiency and transgene expression. Further studies to investigate the timing and duration of prednisolone IS in conjunction with gene therapy may determine whether the observed transient effect can be prolonged.

## MATERIALS AND METHODS

### Animal procedures

All animal care and experimental procedures were approved by the Institutional Animal Care and Use Committee of the University of Pennsylvania and the Children's Hospital of Philadelphia (CHOP). Animals were housed in Association-for-Assessment-and-Accreditation-of-Laboratory-Animal-Care-accredited and Public-Health-Service-assured facilities at CHOP and the University of Pennsylvania.

*Macaca fascicularis* (cynomolgus macaques), sourced from PreLabs (LaBelle, FL), were prescreened for AAV8 NAb as described previously.<sup>42</sup> Twelve adult, sexually mature female and male macaques, ranging from 4.8 to 12.8 years old (body weight 3.4–12.8 kg), with AAV8 NAb titers <1:5, were selected for the study; sexual maturity was determined by animal age. Each animal was randomized according to sex to one of the four treatment groups (n = 3/group: non-IS male or female, prednisolone IS male or female).

In animals randomized to receive IS, oral prednisolone (1 mg/kg/day) was initiated 4 days prior (day –4) to DTX301 administration and continued to day 28. Prednisolone dose was tapered by approximately 25% per week from day 28 to day 56. On day 0, DTX301 (Ultragenyx Pharmaceutical, Novato, CA) was infused to the macaques via the saphenous vein via a Harvard infusion pump (flow rate 2 mL/min) at a dose of  $1.0 \times 10^{13}$  GCs/kg, with dosing volume based on body weight and vector titer. Blood was collected at various time points for different analyses per the study protocol (Figure 1).

On day 28 and day 84 post vector administration, a liver biopsy was performed via laparotomy on each macaque. Necropsy and terminal collection were performed on day 140. Two pieces (one close to the edge and one close to the hilus) from each of the four liver lobes were collected for analyses described hereafter.

### AAV vector

DTX301 is an scAAV8 containing a codon-optimized version of the hOTC coding sequence. The material was made by triple transient transfection of suspension HEK293 cells, with plasmids containing the DTX301 expression cassette, the rep2/cap8 genes, and AdDeltaF6 helper regions. The virus was purified from cell media containing viral particles by AAV8 affinity column chromatography, followed by anion exchange column chromatography. The vector was buffer exchanged into its buffer formulation through tangential flow

filtration. The DTX301 vector was produced by Ultragenyx Gene Therapy. The vector was titered by an optimized qPCR method.

#### Analyses of vector GCs and hOTCco mRNA in liver

Detection and quantification of vector GCs in liver were performed by qPCR using primers and probe designed against the hOTCco transgene sequence of the vector, as previously described.<sup>43</sup> The sensitivity of the assay is 20 GCs/ $\mu$ g DNA or  $1.3 \times 10^{-4}$  GCs/diploid genome. Quantification of transgene mRNA levels was performed by reverse-transcriptase (RT)-qPCR using the same primers and probe set as the vector GC assay, as previously described.<sup>29</sup>

#### ISH

Formalin-fixed, paraffin-embedded liver sections were probed using a ViewRNA In Situ Hybridization Tissue Assay kit (Life Technologies, Carlsbad, CA) following the manufacturer's protocol. Z-shaped probe pairs targeting unintegrated vector DNA and hOTCco mRNA were synthesized by the kit's manufacturer. Hybridized probe pairs were visualized by the deposition of Fast Red substrate, which was imaged with a fluorescence microscope using a rhodamine filter set. Sections were counterstained with DAPI to show nuclei. Quantification of hepatocytes with positive cytoplasm and/or nuclear ISH staining was performed on whole slide images obtained with an Aperio Versa slide scanner (Leica Biosystems, Wetzlar, Germany) using a Visiopharm application (Hoersholm, Denmark).

#### IHC

Paraffin sections were deparaffinized with xylene and ethanol; boiled in a microwave for 6 min in 10 mM citrate buffer (pH 6.0); treated sequentially with 2% H<sub>2</sub>O<sub>2</sub> (15 min; Sigma-Aldrich, St. Louis, MO), avidin/biotin-blocking reagents (15 min each; Vector Laboratories, Burlingame, CA), and blocking buffer (1% donkey serum in phosphate-buffered saline [PBS] + 0.2% Triton for 10 min); followed by incubation with primary (mouse anti-hOTC [clone CL4045; Novus Biologicals NBP2-59038, Littleton, CO]) and biotinylated secondary antibodies (donkey anti-mouse; Jackson ImmunoResearch Laboratories, West Grove, PA) diluted in blocking buffer. A Vectastain Elite ABC kit (Vector Laboratories) was used with 3,3'-diaminobenzidine (DAB) as substrate to visualize bound antibodies as brown precipitate. Sections were slightly counterstained with hematoxylin to show nuclei. OTC deficiency patient control sample was sourced from The National Disease Research Interchange (Philadelphia, PA). Non-study control cynomolgus sample was sourced from a male cynomolgus macaque treated with an unrelated AAV vector. IHC slides were scanned with an Aperio AT2 slide scanner, and the percentage of OTC-positive area on the liver sections was measured using Visiopharm software. The liver from the control animal was used to set a threshold that avoids detection of endogenous OTC.

#### Liver histology

Hematoxylin and eosin staining was performed on sections from paraffin-embedded liver samples; processing and staining were performed according to standard protocols. Liver sections were evaluated

by a board-certified veterinary anatomic pathologist in a blinded manner.

#### IFN $\gamma$ ELISpot assay

Whole blood was collected in heparin tubes for isolation of PBMCs. Lymphocytes were isolated from liver and lymph nodes (axillary, popliteal, and hilar) harvested at terminal biopsy. Isolated lymphocytes were evaluated for IFN  $\gamma$  responses according to previously published methods.<sup>44</sup> Peptide libraries specific for AAV8 capsid and hOTC transgene were generated (15-mer with a 10-amino-acid overlap with the preceding peptide [Mimotopes, VIC, Australia]). More specifically, the AAV8 capsid peptide library was divided into three peptide pools (A, B, and C), and hOTC was split into two peptide pools (A and B). The positive response criteria for the IFN  $\gamma$  ELISpot was arbitrarily defined as greater than 55 spot-forming units per million cells and at least three times greater than the non-stimulated control values.

#### NAb assay

NAb responses against AAV8 were measured in serum using an *in vitro* HEK293 cell-based assay and LacZ-expressing vectors (Vector Core Laboratory, University of Pennsylvania, Philadelphia, PA) as previously described.<sup>44</sup> The NAb titer values are reported as the reciprocal of the highest serum dilution at which AAV transduction is reduced 50% compared with the negative control. The limit of detection of the assay was a 1:5 serum dilution.

#### Vector persistence in the blood

Blood for vector persistence was collected in potassium-EDTA tubes. DNA was extracted from 0.2 mL of whole blood using the QIAamp DNA mini kit (QIAGEN, Germantown, MD) and eluted in a final volume of 40  $\mu$ L. Detection and quantification of vector GC in extracted DNA was performed on 2  $\mu$ L of eluted DNA using the same Taqman assay (Applied Biosystems, Foster City, CA) as for liver vector GC analysis. GCs per milliliter of blood for each sample was extrapolated using a calibrator curve constructed by assaying DNA isolated from naive blood spiked with a range of DTX301 from 0 to  $1 \times 10^{12}$  GCs/mL in 10-fold dilutions.

#### Gene signature analyses

Liver samples were processed to liver lysate using the QuantiGene sample processing kit (Affymetrix, product no. QS0111, Santa Clara, CA) following manufacturer's instructions. Resulting liver lysate was diluted 1:7 with homogenizing solution prior to freezing until branched DNA analysis to assess gene signatures. Control cynomolgus livers were sourced from BioIVT (Westbury, NY).

RNA gene signature analysis was performed using a branched DNA (bDNA) 30-plex panel (Thermo Fisher Scientific, Waltham, MA) designed to assess 21 IFN genes (SPATS2L, EPST11, HERC5, IFI27, IFI44, IFI44L, IFI6, IFIT1B, IFIT3, ISG15, LAMP3, LY6E, MX1, OAS1, OAS2, OAS3, PLSCR1, RSAD2, RTP4, SIGLEC1, and USP18), 5 plasma cell genes (IGHA1, IGJ, IGKC, IGKV4-1, and TNSFR17), and 4 housekeeping genes (PP1B, HPRT1, POLR2A, and GUSB). The GUSB signal was too low in the assay, and its data

were not used. PAXgene blood samples were processed to blood lysate using the QuantiGene sample processing kit following manufacturer's instructions with the following augmentation. PAXgene blood and lysis mixture were incubated at 64°C for 120 min and shaken at 350 rpm. Resulting blood lysate was diluted 1:1 with lysis mixture prior to freezing until bDNA analysis. Control whole cynomolgus blood was sourced from Charles River Laboratories (Reno, NV) and Valley Biosystems (West Sacramento, CA).

The 1:1 diluted blood lysate and 1:7 liver lysate were analyzed using the bDNA kit (Affymetrix, product no. QP1014) and custom 30-plex panel following the manufacturer's instructions for blood lysate. The final plate was read on a Luminex 200 (Luminex, Austin, TX) machine with the following settings (sample size = 100 µL; DD gate = 5,000–25,000; timeout = 105 s; bead region = 50). Bio-Plex manager (Bio-Rad, Hercules, CA) software was used to export the data into an Excel format to be processed for final gene signature results.

The limit of detection (LOD) for each gene was determined for each plate of bDNA analysis by taking the average raw signal of six blank wells and adding three times the standard deviation (SD).

$$LOD = \text{Average of 6 blank wells} + (3 * SD \text{ 6 blank wells})$$

Any sample below the LOD was assigned a value of LOD/2 so each sample had a numerical value. Each gene's signal was then normalized to the geometric mean of the three housekeeping genes (PPIB, HPRT1, and POLR2A). GUSB did not produce a robust signal in the assay and was not used for any purpose.

$$\text{Reported Gene Value} = \frac{\text{Raw Signal}}{\text{GeoMean}(\text{Raw Signal PPIB}, \text{HPRT1}, \text{POLR2A})}$$

Each individual replicate of the well was required to have a minimum bead count of 30. A bead count less than 30 led to a repeat analysis of that sample. Universal NHP RNA control (BioChain, product no. R4534565, Newark, CA) was also plated on each plate at three concentrations (1 µg, 0.5 µg, and 0.1 µg) as an additional plate control to show a change in raw signal in correlation with decreasing concentration.

#### Flow cytometry

The following antibodies were used: CD14 BV510 (clone M5E2), CD16 BV510 (clone 3G8), and CD20 BV510 (clone 2H7) from BioLegend (San Diego, CA); CD4 BUV661 (clone SK3), CD95 BUV737 (clone DX2), CD8 BUV496 (clone RPA-T8), IL-2 APC (clone MQ1-17H12), IFN γ BV750 (clone B27), and CD3 BUV805 (clone SP34-2) from BD Biosciences (San Diego, CA); and TNF-α PE-Cy7 (clone Mab11) from Invitrogen.

Cryopreserved liver or PBMCs were thawed and rested overnight in sterile R10 media (RPMI 1640, Corning), supplemented with 10% fetal

bovine serum (Gemini Bio-Products, West Sacramento, CA), penicillin/streptomycin, and L-glutamine plus 10 U/mL DNase I (Roche Life Sciences, Indianapolis, IN) at 37°C, 5% CO<sub>2</sub>, and 95% humidity incubation conditions. Cells were stimulated as previously described,<sup>45</sup> with a final concentration of 2 mg/mL AAV8 peptide pool C, hOTC peptide pool A or 1 µg/mL Staphylococcal enterotoxin B (SEB) (List Biological Laboratories, Campbell, CA) as a positive control.

After stimulation, cells were washed and stained for viability exclusion using Live/Dead Fixable Aqua (Invitrogen, CA) for 10 min, followed by a 20-min incubation with a panel of directly conjugated monoclonal antibodies diluted in equal parts of fluorescence-activated cell sorting (FACS) buffer (PBS containing 0.1% sodium azide and 1% BSA) and Brilliant stain buffer (BD Biosciences, San Jose, CA). Cells were washed in FACS buffer and fixed and permeabilized using the FoxP3 Transcription Factor Buffer Kit (eBioscience, San Diego, CA), following manufacturer's instructions, and intracellular staining was performed by adding the antibody cocktail prepared in 1× Perm/Wash buffer for 1 h. Stained cells were washed and fixed in PBS containing 1% paraformaldehyde (Sigma-Aldrich). Flow cytometry data were collected on BD FACSymphony A5 cytometer (BD Biosciences). Data were analyzed using FlowJo software (v.10.7.1, Tree Star, Ashland, OR) and GraphPad Prism (v.9.1.0, GraphPad Software, La Jolla, CA).

#### Statistical analysis

GraphPad Prism v.9.1.0 was used for statistical analyses. All values are expressed as mean ± SEM.

To generate heatmaps, values were imported into MORPHEUS (<https://software.broadinstitute.org/morpheus>, Broad Institute, Cambridge, MA). Hierarchical clustering was performed on both rows and columns, without any forced groups, using the “one minus Pearson correlation” metric and the “average” linkage method for hepatic IFN datapoints at days 28 and 84 and endpoint (day 140 or 103; [Figure 5B](#)). Hierarchical clustering was performed only on columns, forcing groups by time (keeping days 103 and 140 together) using the same other parameters for all the blood IFN datapoints ([Figure S9A](#)).

#### SUPPLEMENTAL INFORMATION

Supplemental information can be found online at <https://doi.org/10.1016/j.omtm.2022.01.007>.

#### ACKNOWLEDGMENTS

Funding for this work was provided from Ultragenyx Pharmaceutical Inc. We thank the Nonhuman Primate Program at the Gene Therapy Program (GTP) for animal care and procedures, the Histology Core at

GTP for histology analyses, the Immunology Core for immunology assays, Eric Crombez for providing input during manuscript revision, and the technical assistance of Khadiza Chowdhury. The authors acknowledge the third-party writing assistance of Jack W. Pike and Ellen M. Ross of Envision Pharma Group.

#### AUTHOR CONTRIBUTIONS

L.W., K.M., E.K., S.W., J.M.W., and B.A.S. designed the experiments. L.W., C.C.W., A.K., J.A.C., P.B., Z.H., S.S., E.L.B., M.B.P., M.R.B., J.C., K.M., E.K., J.M.W., S.W., and B.A.S. oversaw and conducted the experiments and performed data analysis. B.A.S. drafted the manuscript.

#### DECLARATION OF INTERESTS

A.K., J.C., K.M., S.W., E.K., and B.A.S. are employees of Ultragenyx Pharmaceutical Inc. J.M.W. is a paid advisor to and holds equity in Scout Bio and Passage Bio; he also has sponsored research agreements with Amicus Therapeutics, Biogen, Elaaj Bio, FA212, Janssen, Passage Bio, and Scout Bio, which are licensees of Penn technology. He also has a sponsored research agreement with G2 Bio. J.M.W. holds equity in the G2-Bio-associated asset companies. J.M.W. and L.W. are inventors on patents that have been licensed to various biopharmaceutical companies and for which they may receive payments.

#### REFERENCES

- Summar, M.L., Koelker, S., Freedenberg, D., Le Mons, C., Haberle, J., Lee, H.S., Kirmse, B., European registry and network for intoxication type metabolic diseases (E-IMD), and members of the urea cycle disorders consortium (UCDC). (2013). The incidence of urea cycle disorders. *Mol. Genet. Metab.* *110*, 179–180.
- Brassier, A., Gobin, S., Arnoux, J.B., Valayannopoulos, V., Habarou, F., Kossorotoff, M., Servais, A., Barbier, V., Dubois, S., Touati, G., et al. (2015). Long-term outcomes in ornithine transcarbamylase deficiency: a series of 90 patients. *Orphanet J. Rare Dis.* *10*, 58.
- Laróvere, L.E., Silvera Ruiz, S.M., Arranz, J.A., and Dodelson de Kremer, R. (2018). Mutation spectrum and genotype–phenotype correlation in a cohort of argentine patients with ornithine transcarbamylase deficiency: a single-center experience. *J. Inborn Errors Metab. Screen.* *6*. <https://doi.org/10.1177/2326409818813177>.
- Wraith, J.E. (2001). Ornithine carbamoyltransferase deficiency. *Arch. Dis. Child.* *84*, 84–88.
- ClinicalTrials.gov (2021). Safety and dose-finding study of DTX301 (scAAV8OTC) in adults with late-onset OTC deficiency (CAPtivate). <https://clinicaltrials.gov/ct2/show/NCT02991144>.
- Wang, L., Morizono, H., Lin, J., Bell, P., Jones, D., McMennamin, D., Yu, H., Batshaw, M.L., and Wilson, J.M. (2012). Preclinical evaluation of a clinical candidate AAV8 vector for ornithine transcarbamylase (OTC) deficiency reveals functional enzyme from each persisting vector genome. *Mol. Genet. Metab.* *105*, 203–211.
- Harding, C.O., Couce, M.L., Geberhiwot, T., Tan, W.-H., Khan, A., Aldamiz-Echevarria, L., Diaz, G.A., Lee, C., Puga, A.C., and Crombez, E. (2021). AAV8 gene therapy as a potential treatment in adults with late-onset ornithine transcarbamylase (OTC) deficiency: updated results from a phase 1/2 clinical trial. *Mol. Ther.* *29*, 17.
- Dauletbekov, D.L., Pfromm, J.K., Fritz, A.K., and Fischer, M.D. (2019). Innate immune response following AAV administration. *Adv. Exp. Med. Biol.* *1185*, 165–168.
- Ronzitti, G., Gross, D.-A., and Mingozzi, F. (2020). Human immune responses to adeno-associated virus (AAV) vectors. *Front. Immunol.* *11*, 670.
- Shirley, J.L., de Jong, Y.P., Terhorst, C., and Herzog, R.W. (2020). Immune responses to viral gene therapy vectors. *Mol. Ther.* *28*, 709–722.
- Kuranda, K., Jean-Alphonse, P., Leborgne, C., Hardet, R., Collaud, F., Marmier, S., Costa Verdera, H., Ronzitti, G., Veron, P., and Mingozzi, F. (2018). Exposure to wild-type AAV drives distinct capsid immunity profiles in humans. *J. Clin. Invest.* *128*, 5267–5279.
- Shirley, J.L., Keeler, G.D., Sherman, A., Zolotukhin, I., Markusic, D.M., Hoffman, B.E., Morel, L.M., Wallet, M.A., Terhorst, C., and Herzog, R.W. (2020). Type I IFN sensing by cDCs and CD4+ T cell help are both requisite for cross-priming of AAV capsid-specific CD8+ T cells. *Mol. Ther.* *28*, 758–770.
- Sack, B.K., and Herzog, R.W. (2009). Evading the immune response upon in vivo gene therapy with viral vectors. *Curr. Opin. Mol. Ther.* *11*, 493–503.
- Chai, Z., Zhang, X., Dobbins, A.L., Rigsbee, K.M., Wang, B., Samulski, R.J., and Li, C. (2019). Optimization of dexamethasone administration for maintaining global transduction efficacy of adeno-associated virus serotype 9. *Hum. Gene Ther.* *30*, 829–840.
- Handyside, B., Zhang, L., Yates, B., Xie, L., Kaplowitz, X., Gorostiza, O., Murphy, R., Fredette, N., Baridon, B., Ngo, K., et al. (2021). The effect of prophylactic corticosteroid treatment on adeno-associated virus (AAV)-mediated gene expression. *Mol. Ther.* *29*, 167.
- Mingozzi, F., and High, K.A. (2017). Overcoming the host immune response to adeno-associated virus gene delivery vectors: the race between clearance, tolerance, neutralization, and escape. *Annu. Rev. Virol.* *4*, 511–534.
- Dane, A.P., Cunningham, S.C., Graf, N.S., and Alexander, I.E. (2009). Sexually dimorphic patterns of episomal rAAV genome persistence in the adult mouse liver and correlation with hepatocellular proliferation. *Mol. Ther.* *17*, 1548–1554.
- Davidoff, A.M., Ng, C.Y.C., Zhou, J., Spence, Y., and Nathwani, A.C. (2003). Sex significantly influences transduction of murine liver by recombinant adeno-associated viral vectors through an androgen-dependent pathway. *Blood* *102*, 480–488.
- Guenzel, A.J., Collard, R., Kraus, J.P., Matern, D., and Barry, M.A. (2015). Long-term sex-biased correction of circulating propionic acidemia disease markers by adeno-associated virus vectors. *Hum. Gene Ther.* *26*, 153–160.
- Nathwani, A.C., Cochrane, M., McIntosh, J., Ng, C.Y.C., Zhou, J., Gray, J.T., and Davidoff, A.M. (2009). Enhancing transduction of the liver by adeno-associated viral vectors. *Gene Ther.* *16*, 60–69.
- Palaschak, B., Herzog, R.W., and Markusic, D.M. (2019). AAV-mediated gene delivery to the liver: overview of current technologies and methods. *Methods Mol. Biol.* *1950*, 333–360.
- Caldovic, L., Abdikarim, I., Narain, S., Tuchman, M., and Morizono, H. (2015). Genotype-phenotype correlations in ornithine transcarbamylase deficiency: a mutation update. *J. Genet. Genomics* *42*, 181–194.
- Smedley, J.V., Bailey, S.A., Perry, R.W., and O'Rourke, C.M. (2002). Methods for predicting sexual maturity in male cynomolgus macaques on the basis of age, body weight, and histologic evaluation of the testes. *Contemp. Top. Lab. Anim. Sci.* *41*, 18–20.
- Park, H.K., Cho, J.W., Lee, B.S., Park, H., Han, J.S., Yang, M.J., Im, W.J., Park, D.Y., Kim, W.J., Han, S.C., et al. (2016). Reference values of clinical pathology parameters in cynomolgus monkeys (*Macaca fascicularis*) used in preclinical studies. *Lab. Anim. Res.* *32*, 79–86.
- Pasi, K.J., Rangarajan, S., Mitchell, N., Lester, W., Symington, E., Madan, B., Laffan, M., Russell, C.B., Li, M., Pierce, G.F., et al. (2020). Multiyear follow-up of AAV5-hFVIII-SQ gene therapy for hemophilia A. *N. Engl. J. Med.* *382*, 29–40.
- Novilla, M.N., Jackson, M.K., Reim, D.A., Jacobson, S.B., and Nagata, R.A. (2014). Occurrence of multinucleated hepatocytes in cynomolgus monkeys (*Macaca fascicularis*) from different geographical regions. *Vet. Pathol.* *51*, 1183–1186.
- Wang, D., Tai, P.W.L., and Gao, G. (2019). Adeno-associated virus vector as a platform for gene therapy delivery. *Nat. Rev. Drug Discov.* *18*, 358–378.
- Rangarajan, S., Walsh, L., Lester, W., Perry, D., Madan, B., Laffan, M., Yu, H., Vettermann, C., Pierce, G.F., Wong, W.Y., et al. (2017). AAV5-factor VIII gene transfer in severe hemophilia A. *N. Engl. J. Med.* *377*, 2519–2530.
- Wang, L., Smith, J., Breton, C., Clark, P., Zhang, J., Ying, L., Che, Y., Lape, J., Bell, P., Calcedo, R., et al. (2018). Meganuclease targeting of PCSK9 in macaque liver leads to stable reduction in serum cholesterol. *Nat. Biotechnol.* *36*, 717–725.
- Konkle, B.A., Walsh, C.E., Escobar, M.A., Josephson, N.C., Young, G., von Drygalski, A., McPhee, S.W.J., Samulski, R.J., Bilic, L., de la Rosa, M., et al. (2021). BAX 335 hemophilia B gene therapy clinical trial results: potential impact of CpG sequences on gene expression. *Blood* *137*, 763–774.

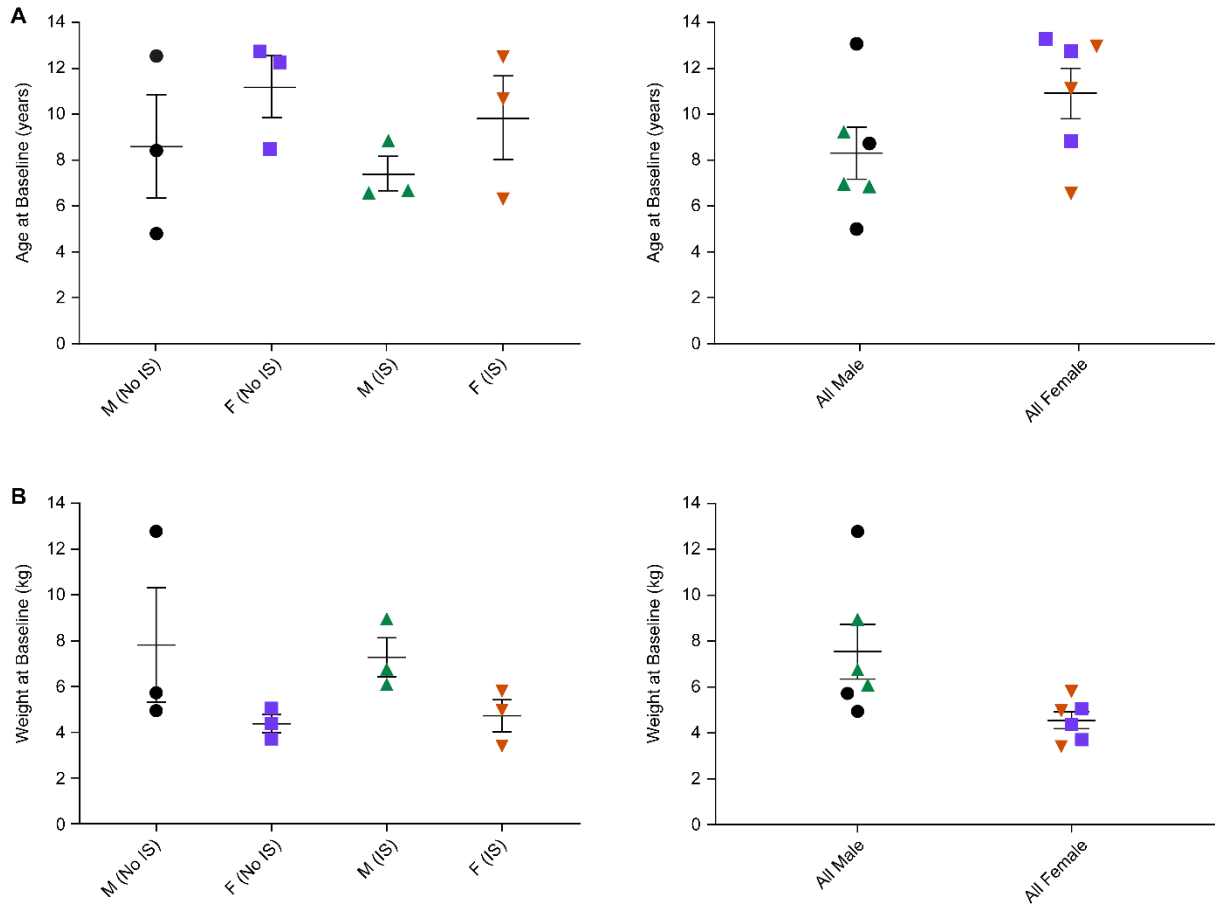
31. Wright, J.F. (2020). Codon modification and PAMPs in clinical AAV vectors: the Tortoise or the hare? *Mol. Ther.* *28*, 701–703.
32. Tsugawa, Y., Kato, H., Fujita, T., Shimotohno, K., and Hijikata, M. (2014). Critical role of interferon- $\alpha$  constitutively produced in human hepatocytes in response to RNA virus infection. *PLoS One* *9*, e89869.
33. Bennett, L., Palucka, A.K., Arce, E., Cantrell, V., Borvak, J., Banchereau, J., and Pascual, V. (2003). Interferon and granulopoiesis signatures in systemic lupus erythematosus blood. *J. Exp. Med.* *197*, 711–723.
34. Gascon-Bayarri, J., Campdelacreu, J., Estela, J., and Rene, R. (2015). Severe hyperammonemia in late-onset ornithine transcarbamylase deficiency triggered by steroid administration. *Case Rep. Neurol. Med.* *2015*, 453752.
35. Lipskind, S., Loanzon, S., Simi, E., and Ouyang, D.W. (2011). Hyperammonemic coma in an ornithine transcarbamylase mutation carrier following antepartum corticosteroids. *J. Perinatol.* *31*, 682–684.
36. Löfberg, E., Gutierrez, A., Wernerman, J., Anderstam, B., Mitch, W.E., Price, S.R., Bergström, J., and Alvestrand, A. (2002). Effects of high doses of glucocorticoids on free amino acids, ribosomes and protein turnover in human muscle. *Eur. J. Clin. Invest.* *32*, 345–353.
37. Maier, K.P., Talke, H., Heimsoeth, H., and Gerok, W. (1978). Influence of steroids on urea-cycle enzymes in chronic human liver disease. *Klin. Wochenschr.* *56*, 291–295.
38. Summar, M.L., Barr, F., Dawling, S., Smith, W., Lee, B., Singh, R.H., Rhead, W.J., Sniderman King, L., and Christman, B.W. (2005). Unmasked adult-onset urea cycle disorders in the critical care setting. *Crit. Care Clin.* *21*, S1–S8.
39. Klein, S.L., and Flanagan, K.L. (2016). Sex differences in immune responses. *Nat. Rev. Immunol.* *16*, 626–638.
40. Baruteau, J., Cunningham, S.C., Yilmaz, B.S., Perocheau, D.P., Eaglestone, S., Burke, D., Thrasher, A.J., Waddington, S.N., Lisowski, L., Alexander, I.E., et al. (2021). Safety and efficacy of an engineered hepatotropic AAV gene therapy for ornithine transcarbamylase deficiency in cynomolgus monkeys. *Mol. Ther. Methods Clin. Dev.* *23*, 135–146.
41. Binny, C., McIntosh, J., Della Peruta, M., Kymalainen, H., Tuddenham, E.G.D., Buckley, S.M.K., Waddington, S.N., McVey, J.H., Spence, Y., Morton, C.L., et al. (2012). AAV-mediated gene transfer in the perinatal period results in expression of FVII at levels that protect against fatal spontaneous hemorrhage. *Blood* *119*, 957–966.
42. Calcedo, R., Vandenberghe, L.H., Gao, G., Lin, J., and Wilson, J.M. (2009). Worldwide epidemiology of neutralizing antibodies to adeno-associated viruses. *J. Infect. Dis.* *199*, 381–390.
43. Bell, P., Moscioni, A.D., McCarter, R.J., Wu, D., Gao, G., Hoang, A., Sanmiguel, J.C., Sun, X., Wivel, N.A., Raper, S.E., et al. (2006). Analysis of tumors arising in male B6C3F1 mice with and without AAV vector delivery to liver. *Mol. Ther.* *14*, 34–44.
44. Calcedo, R., Chichester, J.A., and Wilson, J.M. (2018). Assessment of humoral, innate, and t-cell immune responses to adeno-associated virus vectors. *Hum. Gene Ther. Methods* *29*, 86–95.
45. Greig, J.A., Calcedo, R., Kuri-Cervantes, L., Nordin, J.M.L., Albrecht, J., Bote, E., Goode, T., Chroscinski, E.A., Bell, P., Richman, L.K., et al. (2018). AAV8 gene therapy for crigler-najjar syndrome in macaques elicited transgene T cell responses that are resident to the liver. *Mol. Ther. Methods Clin. Dev.* *11*, 191–201.

**Supplemental information**

**Prednisolone reduces the interferon  
response to AAV in cynomolgus macaques  
and may increase liver gene expression**

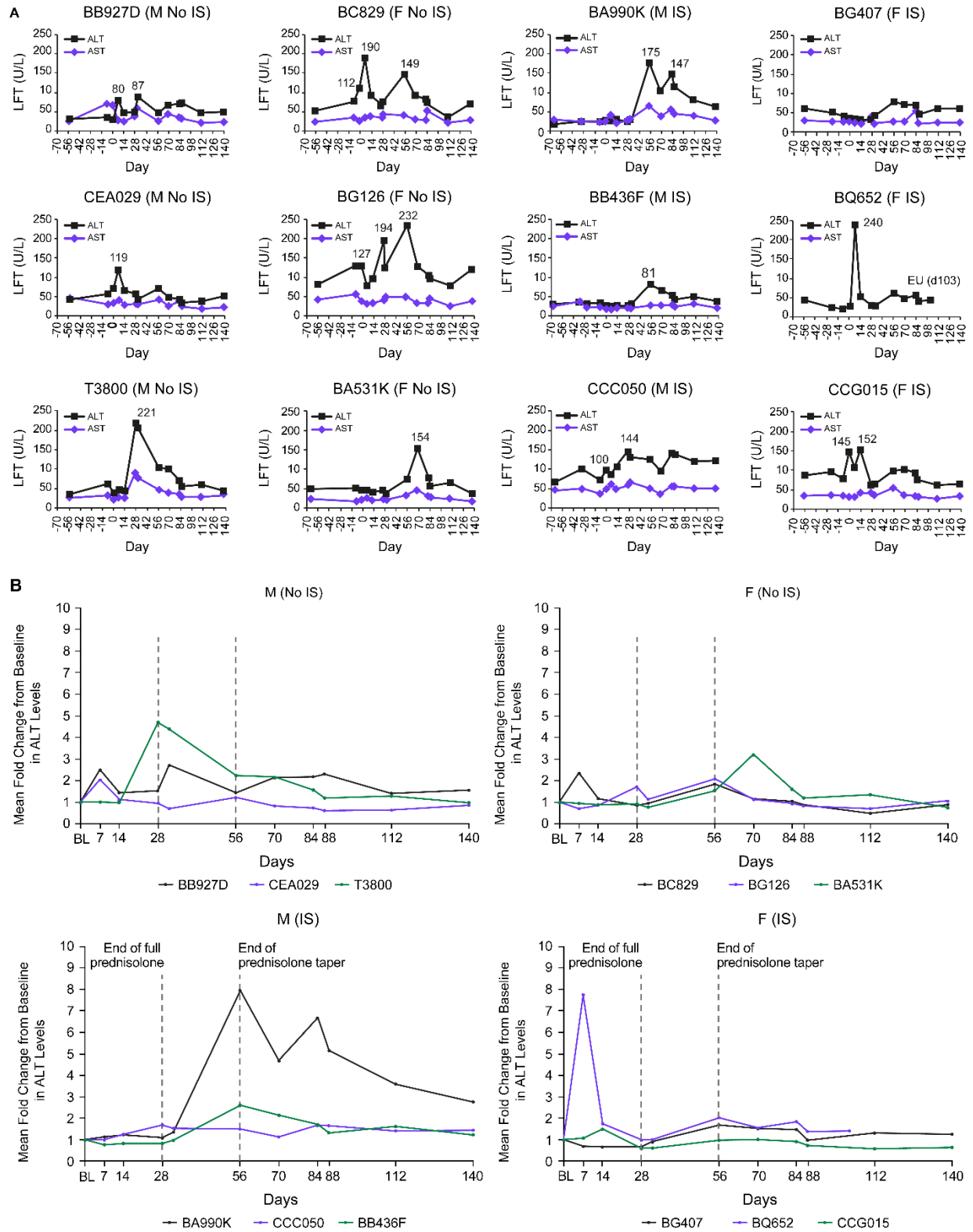
**Lili Wang, Claude C. Warzecha, Alexander Kistner, Jessica A. Chichester, Peter Bell, Elizabeth L. Buza, Zhenning He, M. Betina Pampena, Julien Couthouis, Sunjay Sethi, Kathleen McKeever, Michael R. Betts, Emil Kakkis, James M. Wilson, Samuel Wadsworth, and Barbara A. Sullivan**

## Supplemental Data



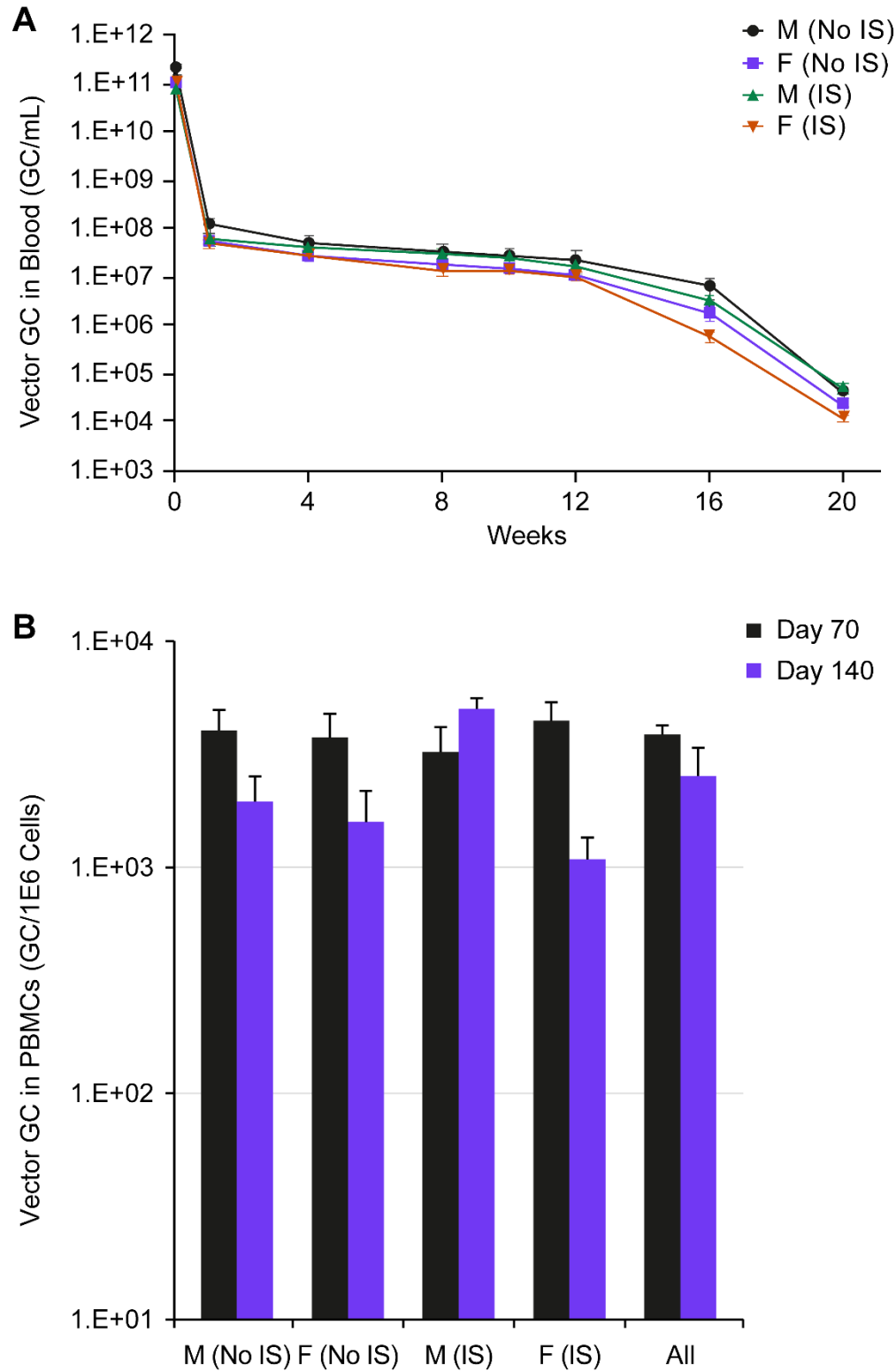
**Figure S1. Age and weight at baseline according to study group and sex.** (A) Age and (B) weight at baseline for individual macaques is shown per study group (left panels) and by sex (right panels). Data are represented as individual values for each animal with mean  $\pm$  SEM. F, female; IS, immunosuppression; M, male.



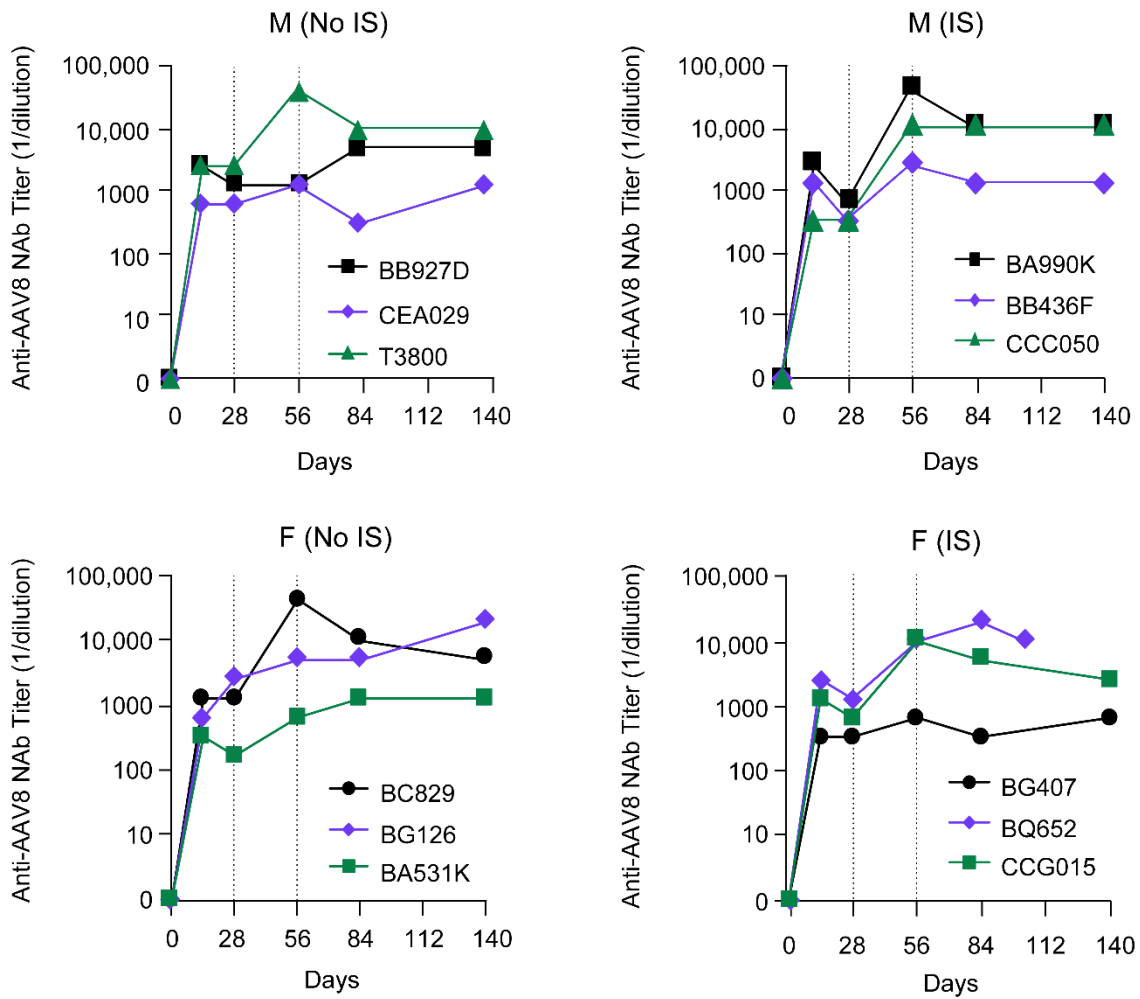


**Figure S2. Alanine aminotransferase and aspartate aminotransferase levels in non-human primates (NHPs) following DTX301 administration.** (A) Alanine aminotransferase (ALT) and aspartate aminotransferase (AST) levels were quantified in individual macaques at the indicated time points. (B) ALT levels shown as fold change

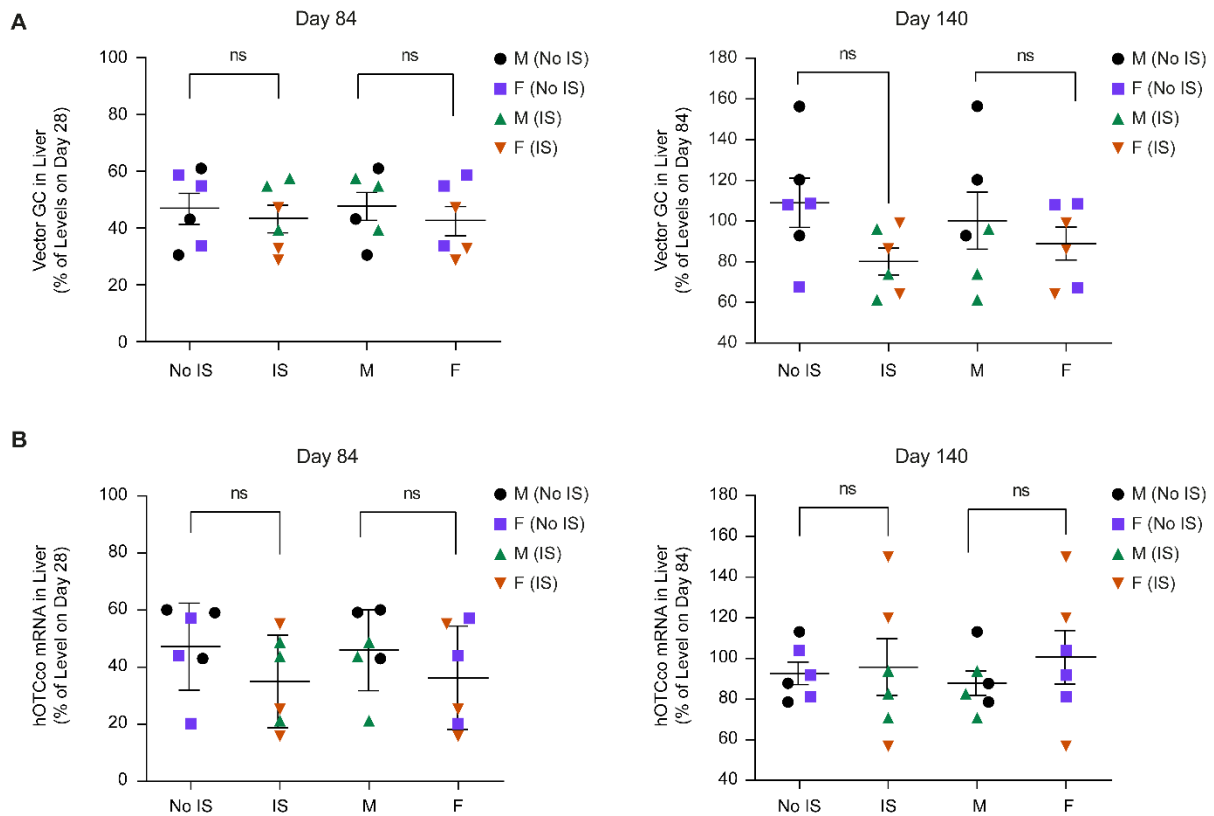
from baseline for individual cynomolgus macaques by treatment group. F, female; IS, immunosuppression; LFT, liver function test; M, male.



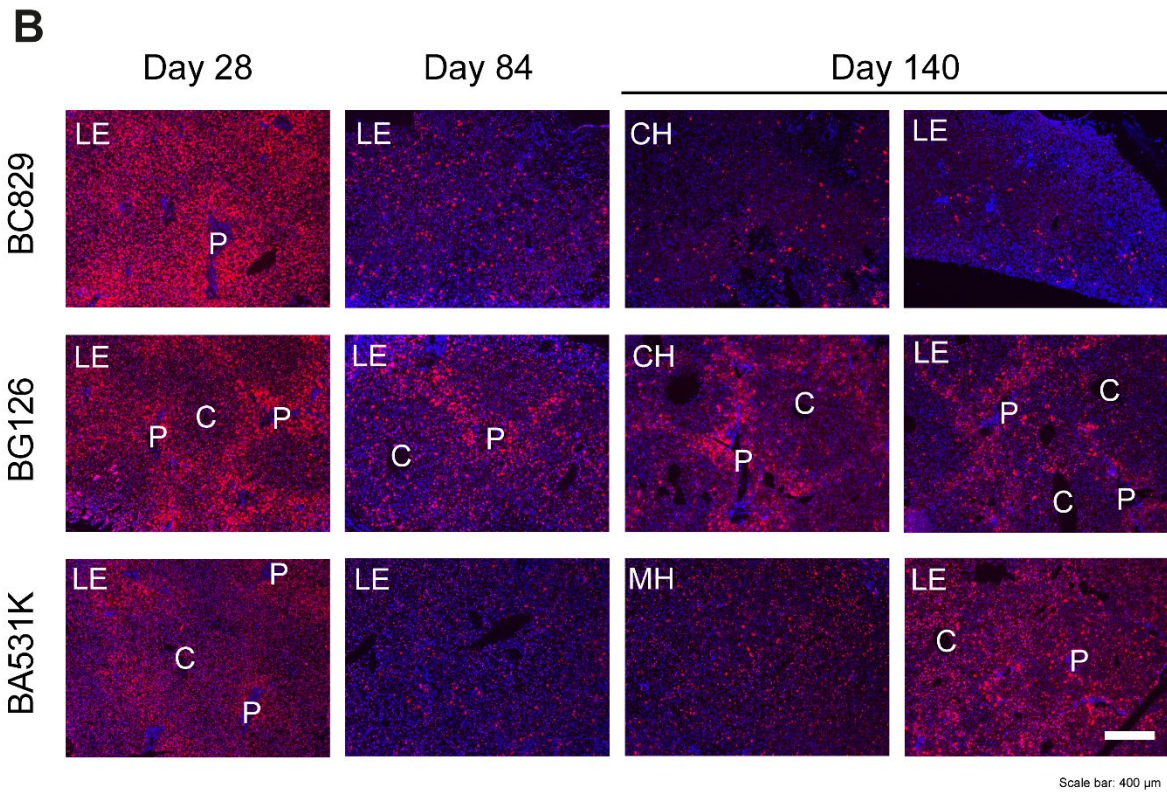
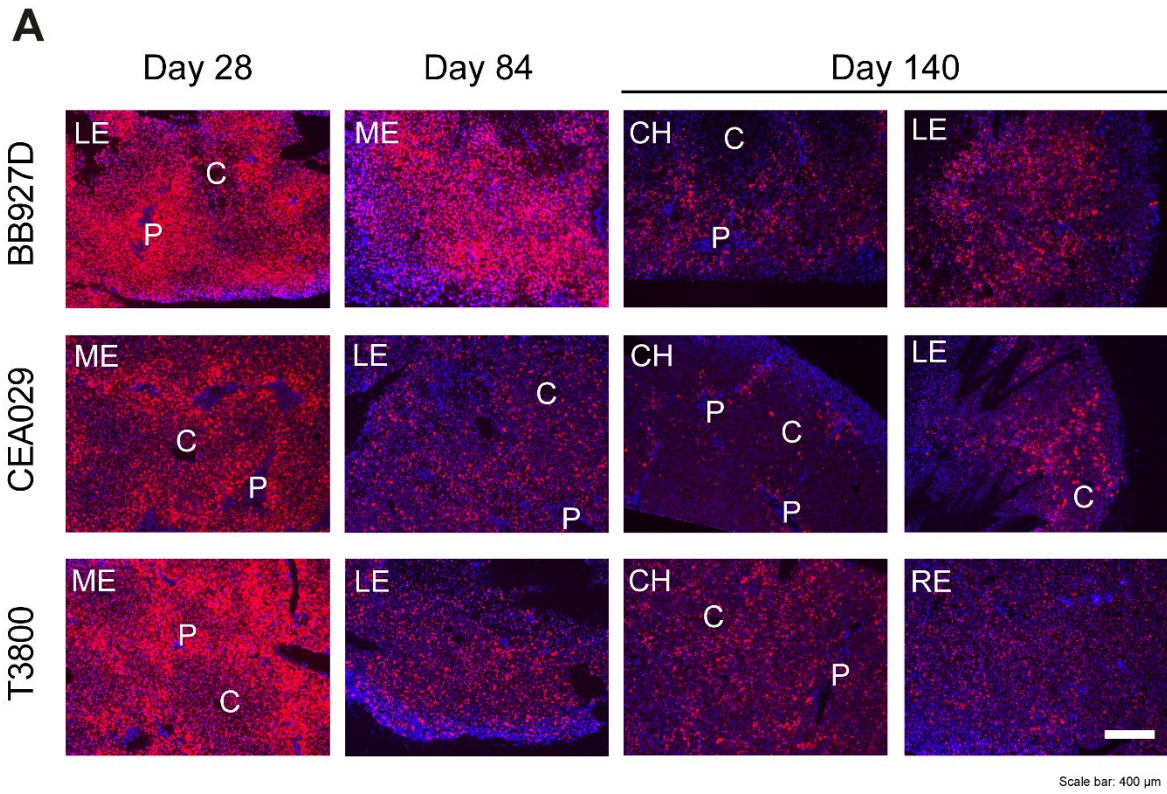
**Figure S3. Vector DNA expression in the blood.** Vector DNA levels were quantified in the blood of individual macaques by quantitative polymerase chain reaction (qPCR) at the indicated time points. (A) Vector DNA in whole blood. Data are represented as the mean  $\pm$  SEM for each treatment group. (B) Vector DNA in peripheral blood mononuclear cells (PBMCs). Data are represented as mean  $\pm$  SEM for each treatment group and for all animals. F, female; GC, genome copies; IS, immunosuppression; M, male.

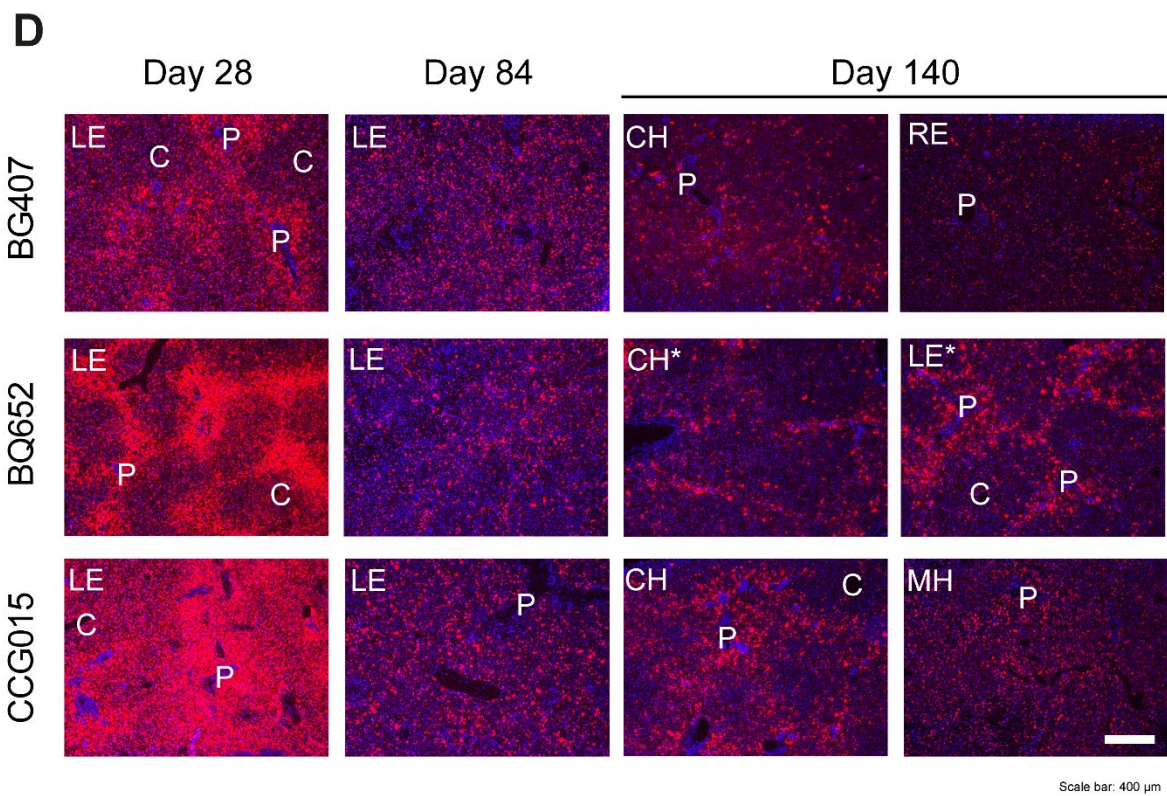
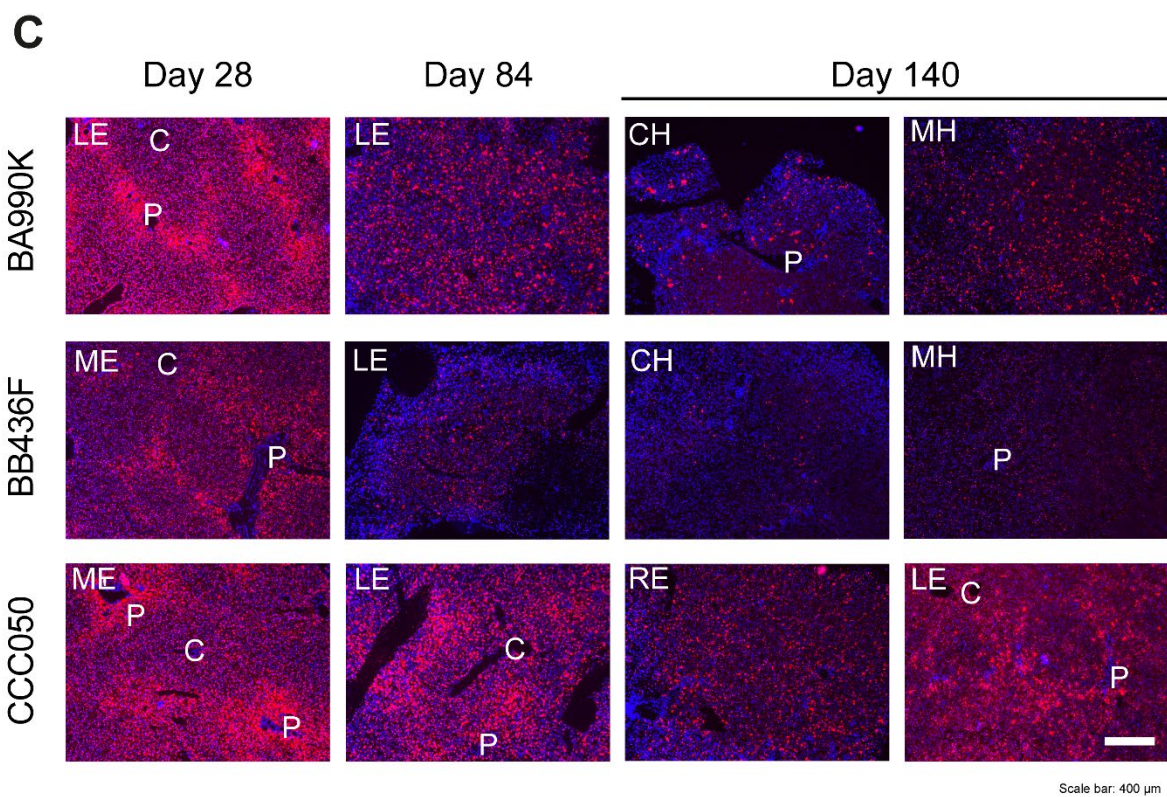


**Figure S4. Neutralizing antibody assay responses following DTX301 administration in NHP with or without immunosuppression.** Serum anti-AAV8 neutralizing antibody (NAb) titers were evaluated in individual cynomolgus macaques at the indicated time points using a cell-based neutralization assay. The NAb titer values are reported as the reciprocal of the highest serum dilution at which AAV transduction is reduced 50% compared to the negative control. F, female; IS, immunosuppression; M, male.



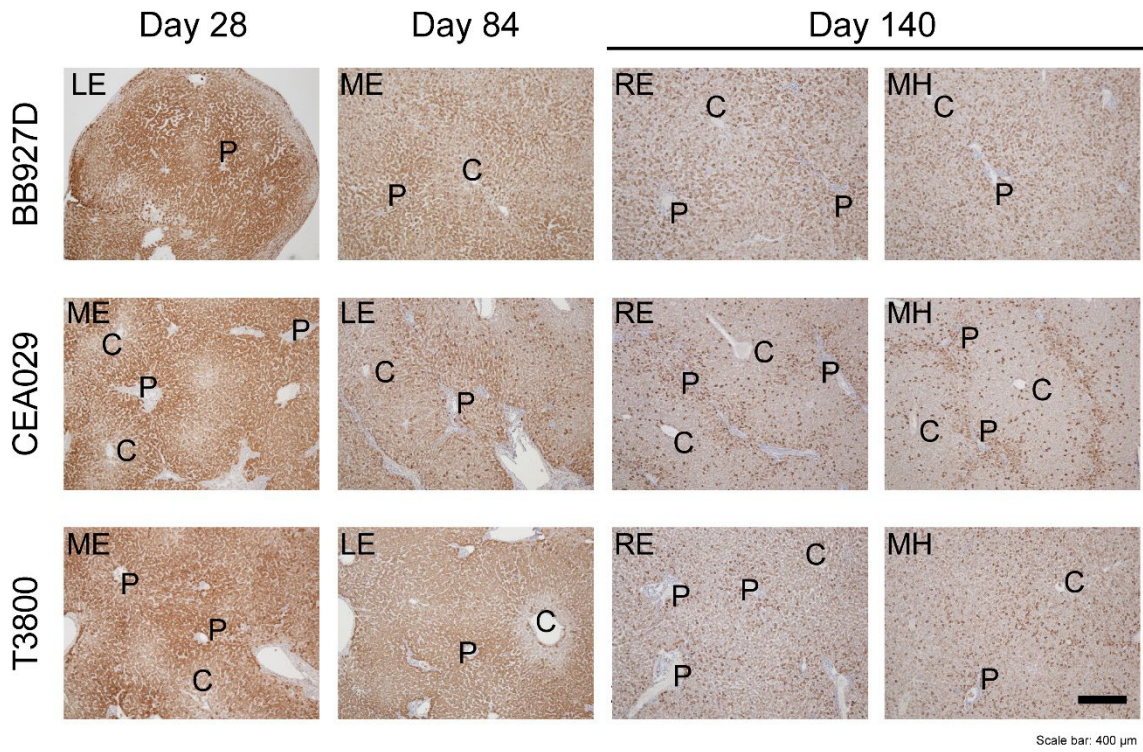
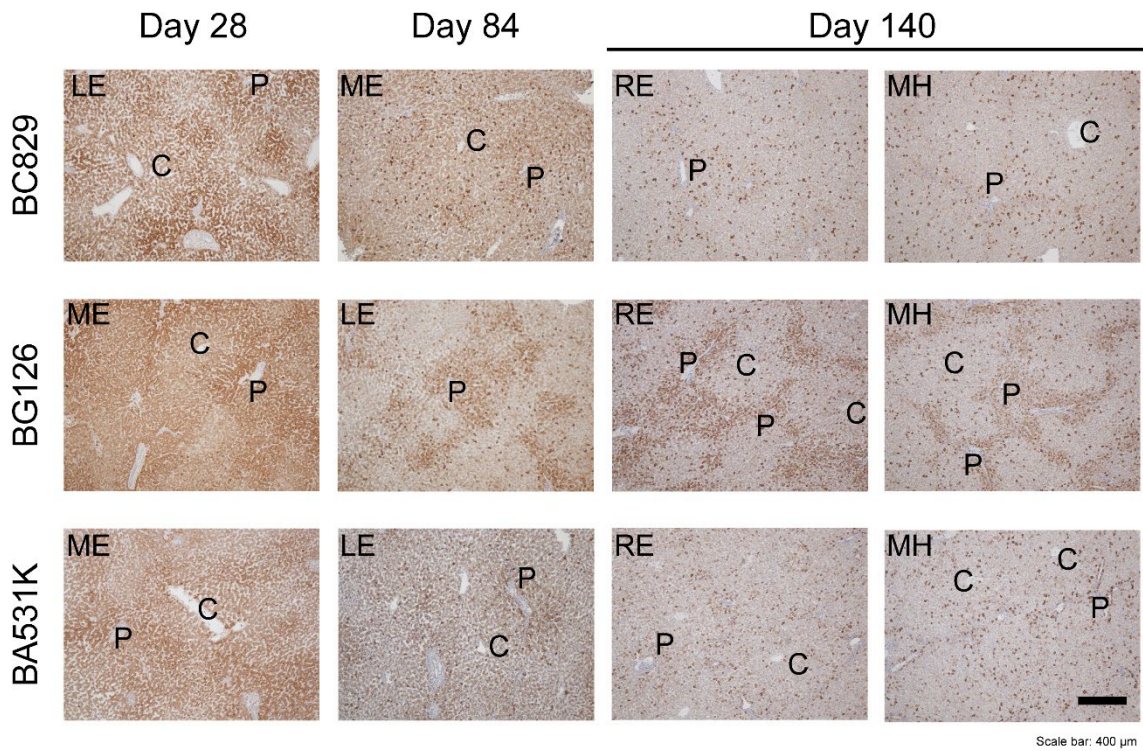
**Figure S5. Change of vector genome copies and human codon-optimized OTC messenger RNA levels over time in liver.** (A) Vector DNA and (B) human codon-optimized OTC (hOTCco) messenger (m)RNA levels were quantified in liver biopsies of individual cynomolgus macaques at day 84 and day 140. For each NHP, vector genome copies (GC) and hOTCco mRNA levels in liver on day 84 (left panel) and day 140 (right panel) are presented as the proportion of the levels on the previous time points (day 28 and day 84, respectively). Data are represented as individual values for each animal with mean  $\pm$  SEM. Statistical analysis was performed using a Mann-Whitney test. ns, not significant. F, female; GC, genome copies; IS, immunosuppression; M, male. See also Figure 2.

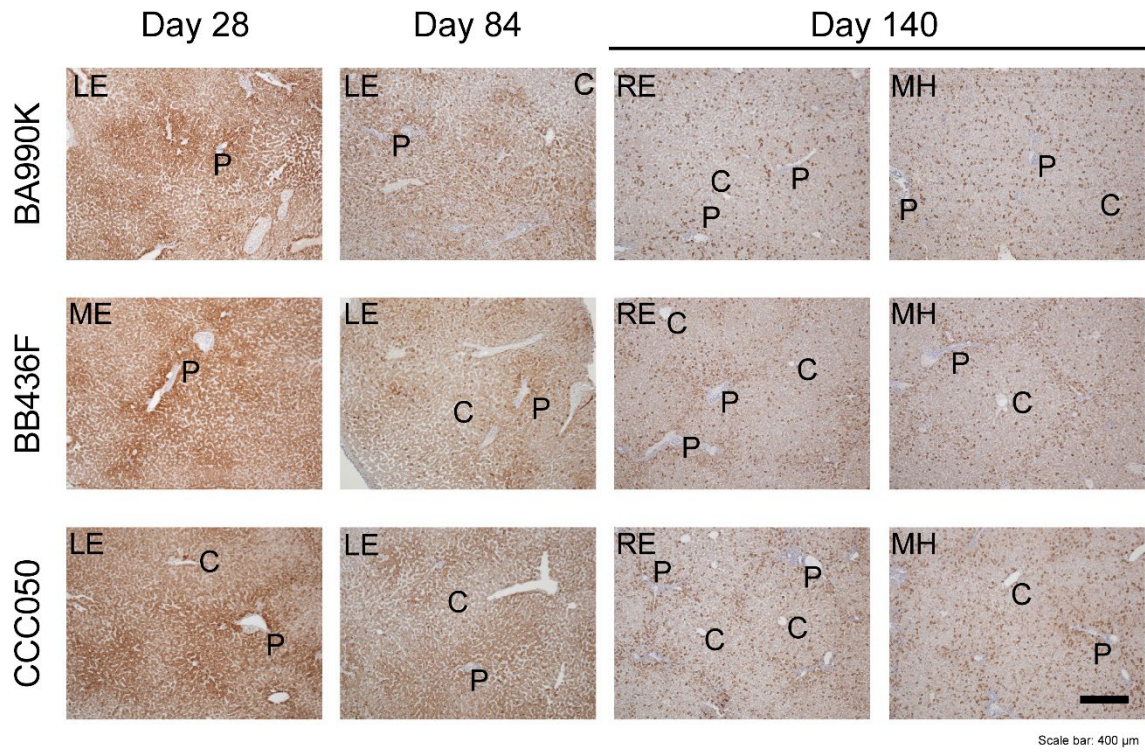
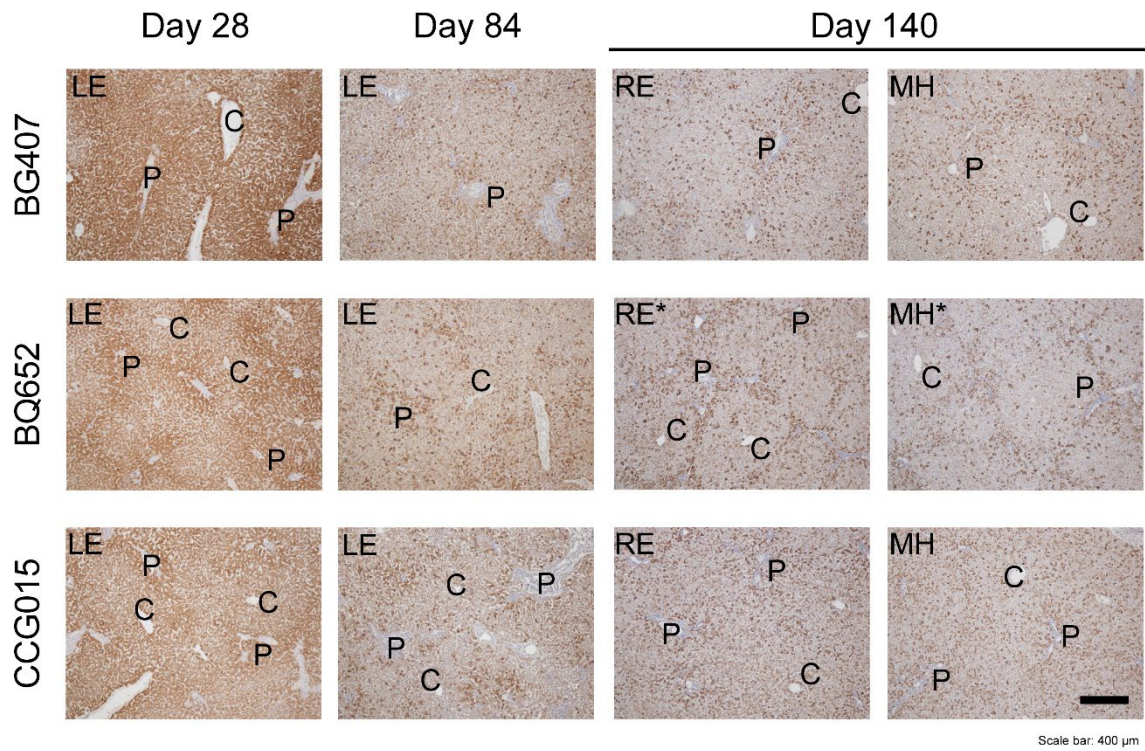




**Figure S6. hOTCco expression in the liver by In Situ Hybridization.** Transgene expression by hepatocytes was analyzed in liver sections of individual cynomolgus macaques for (A) M (No IS), (B) F (No IS), (C) M (IS) and (D) F (IS) by performing In Situ Hybridization (ISH) at day 28, day 84 and day 140. ISH images (4x) are shown for each animal. Central areas are labelled with C and portal regions are labelled with P. Scale bar indicates 400  $\mu$ m. \*ISH images for animal BQ652 are from day 103 when this animal was necropsied. CH, caudate hilus; F, female; IS, immunosuppression; LE, left edge; M, male; ME, medial edge; MH, medial hilus; RE, right edge. See also Figure 3 and Figure S8.



**A****B**

**C****D**

**Figure S7. hOTC expression in the liver by immunohistochemistry.** Transgene expression by hepatocytes was analysed in liver sections of individual cynomolgus macaques for (A) M (No IS), (B) F (No IS), (C) M (IS) and (D) F (IS) by performing IHC at day 28, day 84 and day 140. IHC images (4x) are shown for each animal. Central areas are labelled with C and portal regions are labelled with P. Scale bar indicates 400  $\mu\text{m}$ . \*IHC images for animal BQ652 are from day 103 when this animal was necropsied. F, female; IS, immunosuppression; LE, left edge; M, male; ME, medial edge; MH, medial hilus; RE, right edge. See also Figure 4.

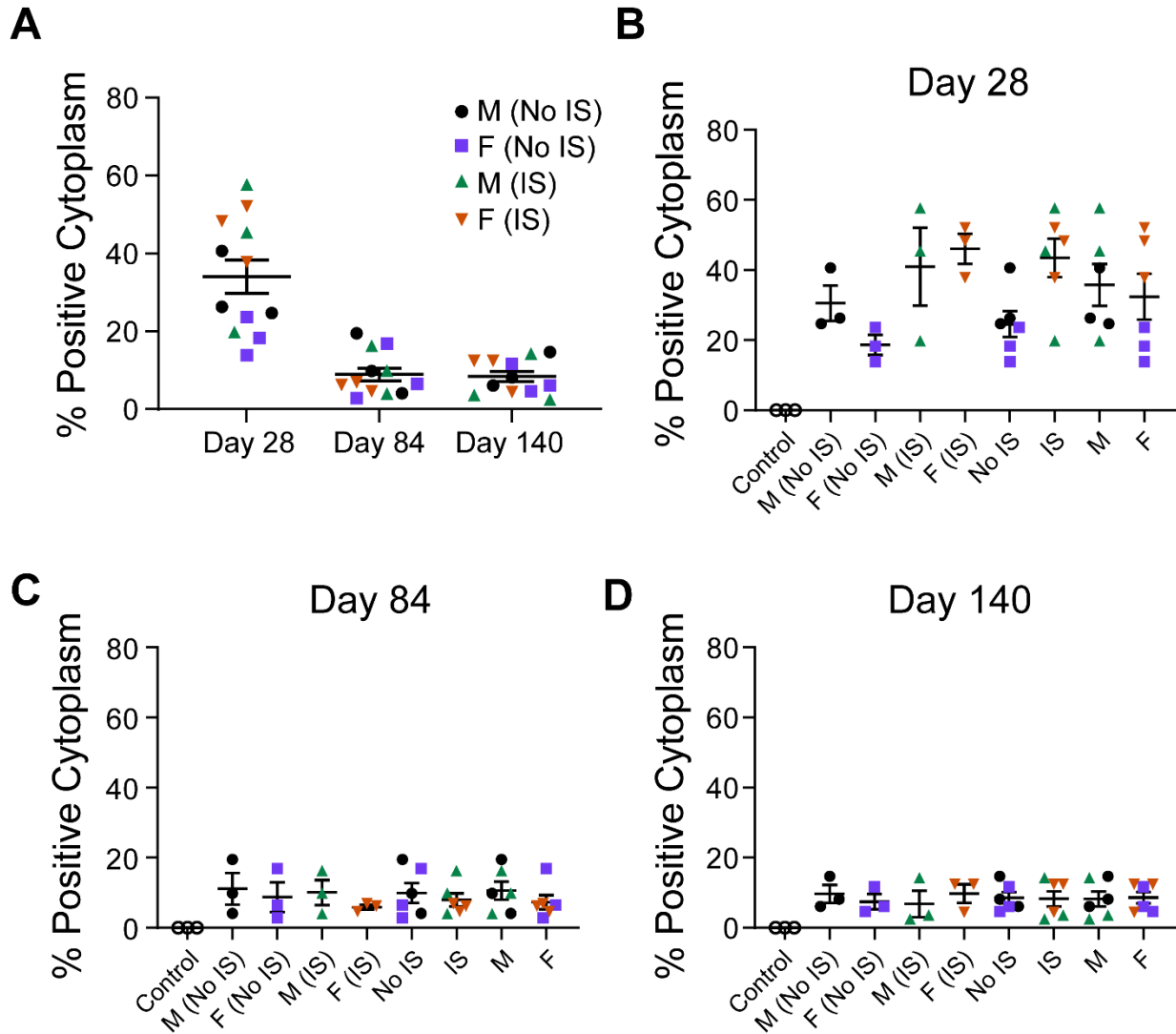


**Figure S8. hOTCco expression in the liver at different time points by In Situ Hybridization.** Transgene expression by hepatocytes was analyzed in liver sections of individual cynomolgus macaques by performing In Situ Hybridization (ISH) at day 28, day 84 and day 140. hOTCco expression was analyzed using computer morphology analysis. Proportion of hepatocytes with positive cytoplasm is shown by day (A) and for individual groups (B – D). For day 28 and day 84, data are represented as individual values for each animal with mean  $\pm$  SEM. For day 140, data are represented as the mean of 2 lobe values for each animal with mean  $\pm$  SEM. F, female; IS, immunosuppression; M, male. See also Figure 3 and Figure S6.

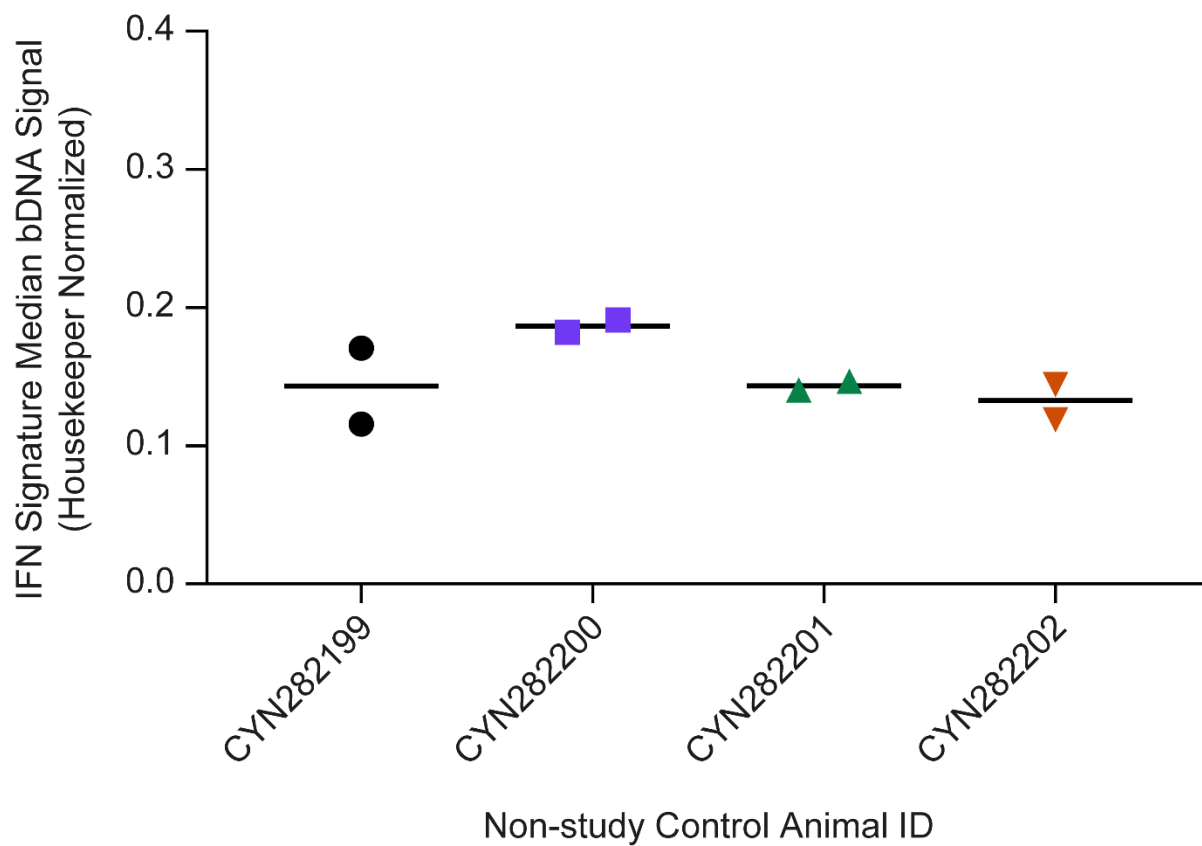


**Figure S9. Inter-lobe IFN signature concordance within control liver samples.** The hepatic IFN gene signature was evaluated in 4 control cynomolgus macaques by determining the expression of 21 IFN-driven genes in liver lysates using a branched (b)DNA assay. Shown is the median IFN signature bDNA signal normalized to expression of housekeeping genes for the left and right liver lobes (mean shown as horizontal lines). See also Figure 5.

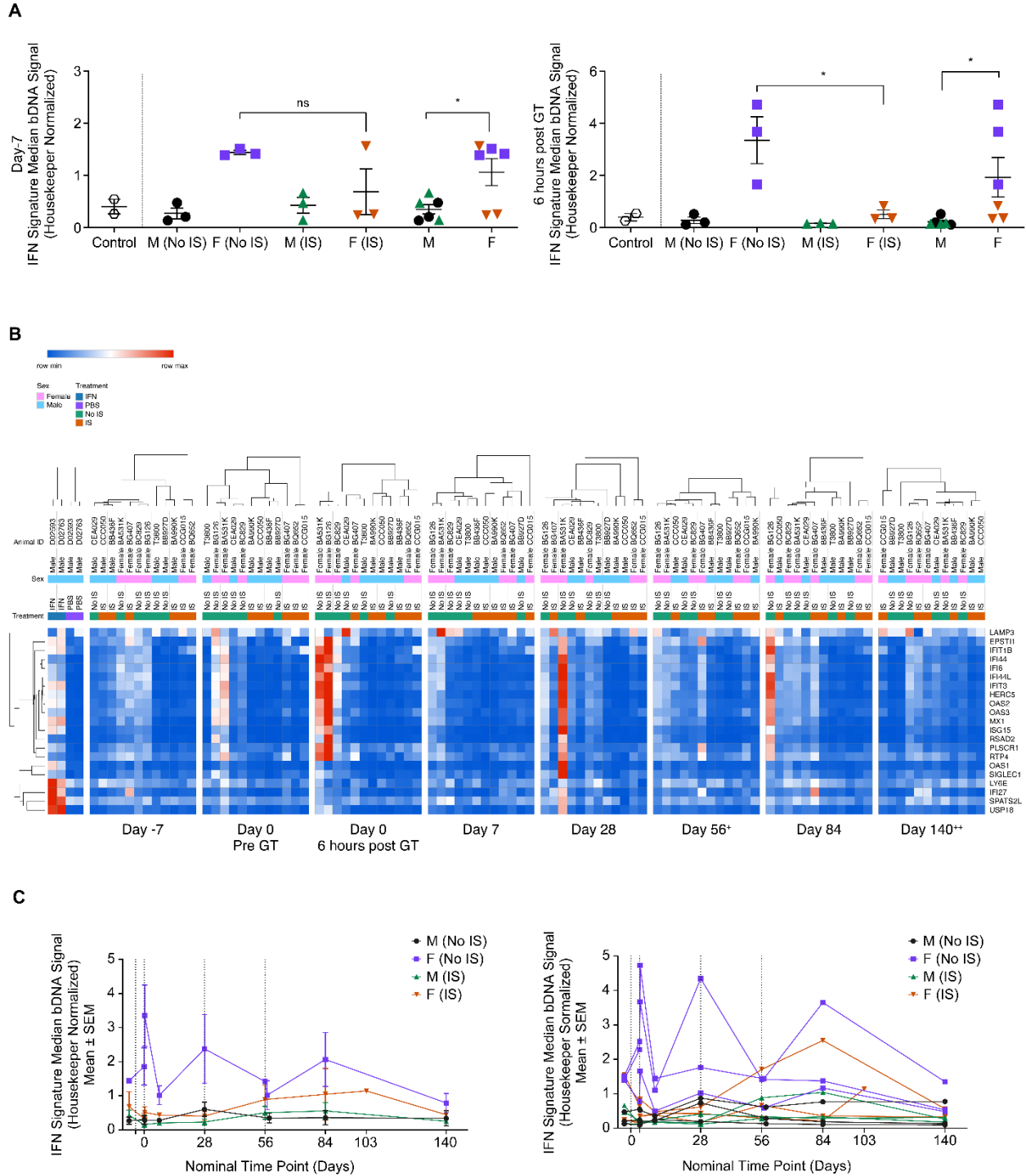


**Figure S10. Analysis of blood IFN signature.** The blood IFN gene signature was evaluated in individual cynomolgus macaques by determining the expression of 21 IFN-driven genes in whole blood using a bDNA assay. (A) Blood IFN gene signature by group at day -7 (left panel) and day 0 (6 hours post-vector administration) (right panel) for the study animals alongside non-study control blood samples. Data are represented as mean  $\pm$  SEM of the median IFN signature bDNA signal normalized to expression of housekeeping for each animal. (B) Blood IFN gene signature heatmaps showing all 21 genes at day 0 (pre- and 6 hours post-vector administration), day 7, day 28, day 56, day 84 and day 140. +Animal BG126 and BC829 evaluated at day 57; animal CEA029, T3800 and BB927D

evaluated at day 58. <sup>††</sup>Animal BQ652 evaluated at day 103. (C) Blood IFN gene signature at the indicated time points. Left panel: data are represented as mean  $\pm$  SEM of the median IFN signature bDNA signal for each group. Right panel: median IFN signature bDNA signal for individual animals. Statistical analysis was performed using an unpaired t test. ns, not significant,  $*P < 0.05$ . F, female; GT, gene therapy; IS, immunosuppression; M, male. See also Figure S11.

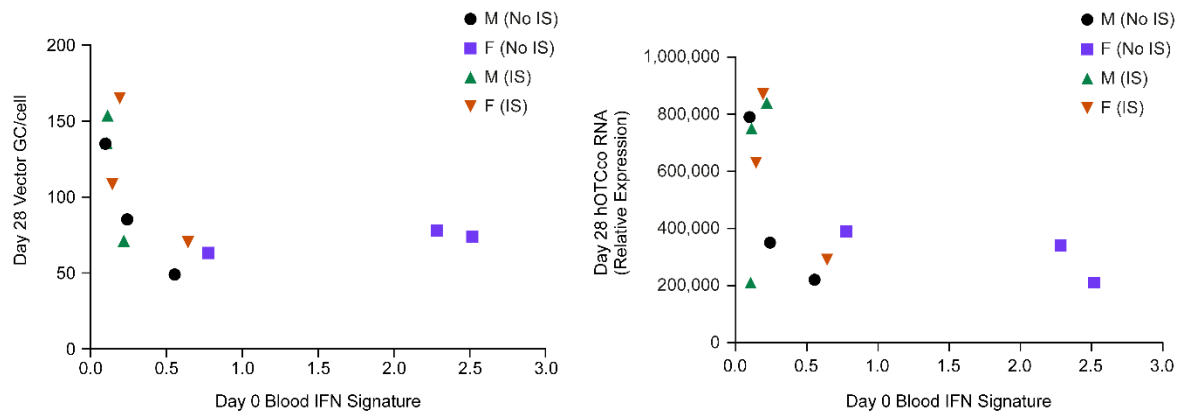


**Figure S11. Analysis of baseline blood IFN signature with liver vector GC/cell and hOTCco mRNA at day 28.** The blood IFN gene signature of individual macaques at baseline (day 0) was plotted against vector DNA (left panel) and hOTCco mRNA (right panel) at day 28. See also Figure S9. F, female; GC, genome copies; IS, immunosuppression; M, male. See also Figure S10.



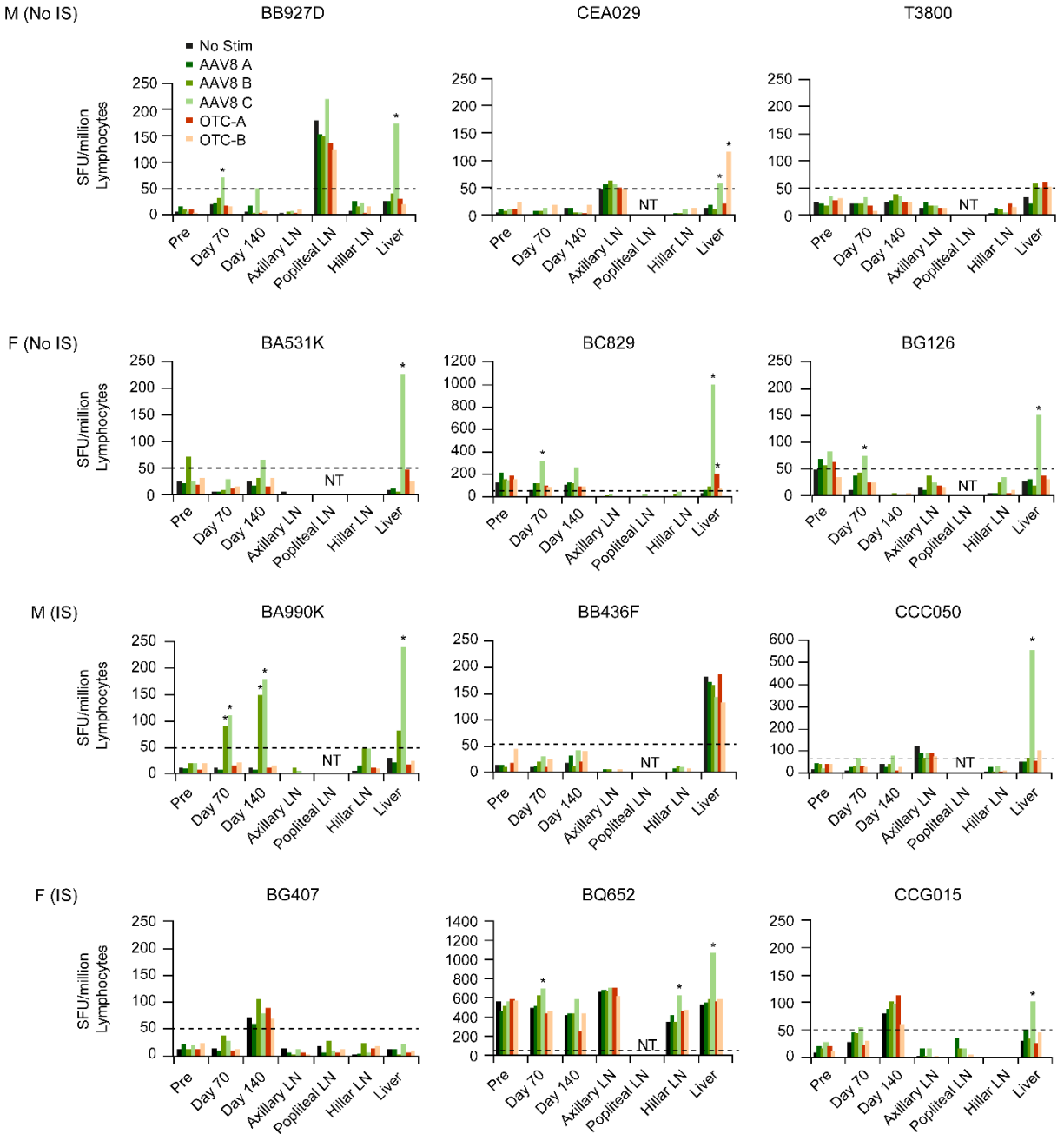


**Figure S12. ELISpot analysis of liver lymphocytes and control tissues.** The IFN  $\gamma$  cellular response to AAV8 capsid and hOTC protein was evaluated in PBMCs, lymph nodes (axillary, popliteal, and hilar), and the liver of individual cynomolgus macaques by IFN  $\gamma$  ELISpot. PBMCs were analysed at baseline (day -7), day 70 and day 140; lymph nodes and liver were analysed at day 140 (animal BQ652 was euthanized before study end and was evaluated at day 103). The AAV8 capsid peptide library was divided into 3 peptide pools (A, B, and C) and hOTC was split into 2 peptide pools (A and B). \* indicates positive response which is arbitrarily defined as greater than 55 spot-forming units (SFU) per million cells and at least 3 times greater than the non-stimulated control values. F, female; IS, immunosuppression; LN, lymph node; M, male; NT, not tested.

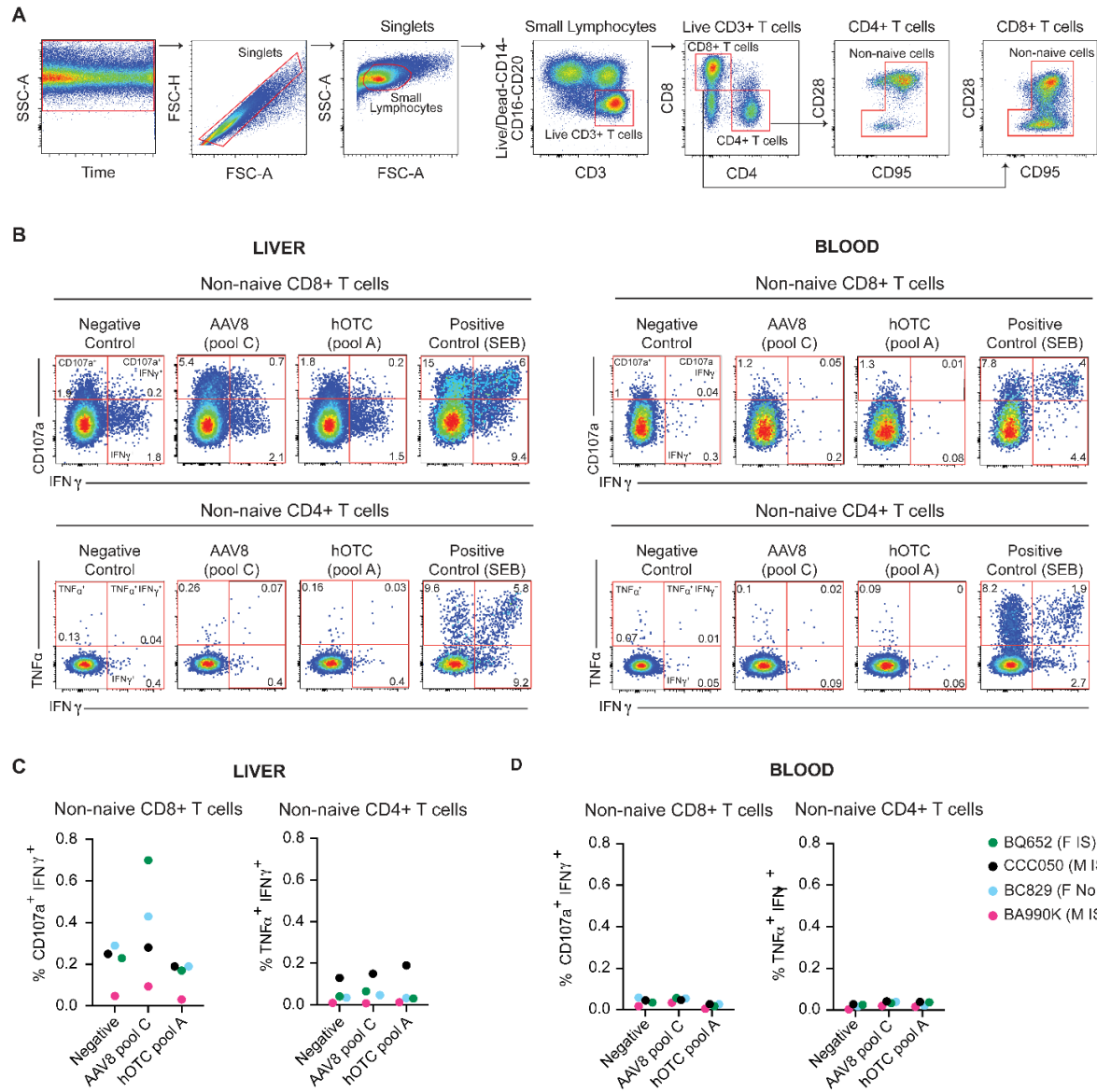


**Figure S13. Flow cytometric analysis of liver and blood T cells from animals showing elevated ELISpot counts.** (A) Representative flow plots showing the gating strategy used to analyze T cell responses. The most stable acquisition was first selected. Forward scatter height (FSC-H)-versus-forward scatter area (FSC-A) and side scatter area (SSC-A)-versus-FSC-A plots were used to exclude doublets and focus on singlet small lymphocytes. Dead cells were excluded by gating on cells negative for the viability marker Aqua Blue. Monocytes, B cells and NK cells were excluded via the CD14/20/16 dump gate. CD4+ and CD8+ T lymphocytes were gated within CD3+ cells. To determine the memory phenotype, CD28 versus CD95 were used, and naïve T cells (CD28+CD95-) were excluded from the analysis. (B) Flow cytometry plots from cynomolgus BQ652 showing, for each condition, the frequency of CD107a+ or IFN $\gamma$ + or double positive CD107a+IFN $\gamma$ + cells within non-naïve CD8+ T cells; and TNF $\alpha$ + or IFN $\gamma$ + or double positive TNF $\alpha$ +IFN $\gamma$ + cells within non-naïve CD4+ T cells in liver or blood at day 103. The numbers indicate the frequency within the parent population. (C) Collated data showing the CD8+ and CD4+ T cell responses against AAV8 peptide pool C and hOTC peptide pool A in liver at day 103 for cynomolgus BQ652 or at day 140 for BA990K, BC829 and CCC050. (D) Collated data showing the CD8+ and CD4+ T cell responses against AAV8 peptide pool C and hOTC peptide pool A in blood at day 103 for cynomolgus BQ652 or at day 140 for BA990K, BC829 and CCC050. SEB, Staphylococcus Enterotoxin B.

**Table S1:** Cellular composition of liver samples at Days 28, 84, and 140.

<b>Biopsy 1</b>	<b>Day 28</b>			
Immunosuppression	Control (none)		Prednisolone	
Sex	Male	Female	Male	Female
Number of animals evaluated per group	3	3	3	3
Liver				
No. examined	3	3	3	3
No. abnormalities detected	0	0	2	0
Infiltrate; mononuclear cell				
Grade 1	-	3	1	2
Grade 2	2	-	-	1
Necrosis; individual hepatocellular, periportal				
Grade 1	1	-	-	-
Hypertrophy; hepatocellular, with dissociation, diffuse				
Grade 1	-	-	-	1
Multinucleation; hepatocellular, centrilobular, focal				
Grade 1	-	-	-	1
Fibrosis; capsule, regional				
Grade 1	-	1	-	1
Grade 2	1	-	-	-
Fibrosis; capsule and subcapsular, regional				
Grade 3	-	1	-	-
Decreased, portal and centrilobular areas; focally extensive				
Grade 2	1	-	-	-
<b>Biopsy 2</b>	<b>Day 84</b>			
Immunosuppression	Control (none)		Prednisolone	
Sex	Male	Female	Male	Female
Number of animals evaluated per group	3	3	3	3
Liver				
No. examined	3	3	3	3
No. abnormalities detected	0	0	0	0
Infiltrate; mononuclear cell				
Grade 1	1	3	3	-
Grade 2	1	-	-	1
Grade 3	-	-	-	1
Necrosis; individual hepatocellular, periportal				
Grade 1	-	-	-	1
Multinucleation; hepatocellular, multifocal				
Grade 2	1	-	-	2
Fibrosis; capsule, regional				
Grade 1	-	-	1	-
Fibrosis; capsule, diffuse				
Grade 2	2	-	1	-
Fibrosis; capsule and subcapsular, regional				

Grade 3	-	-	-	1
Decreased, portal and centrilobular areas; focally extensive				
Grade 4	1	-	-	1
Decreased, lobular size; subcapsular, regional				
Grade 2	-	-	-	1
<b>Necropsy</b>				
	<b>Day 140<sup>a</sup></b>			
Immunosuppression	Control (none)		Prednisolone	
Sex	Male	Female	Male	Female
Number of animals evaluated per group	3	3	3	3 <sup>a</sup>
Liver (Necropsy)				
No. liver lobes examined (hilus and edge sections for caudate, left, middle, right)	24	24	24	24
No. abnormalities detected	0	0	0	0
Infiltrate; mononuclear cell				
Grade 1	5	1	4	-
Grade 2	19	23	20	24 <sup>a</sup>
Multinucleation; hepatocellular, multifocal				
Grade 2	1	-	6	-
Fibrosis/fibrovascular tissue; capsule +/- subcapsular				
Grade 1	5	9	4	10
Grade 2	3	2	1	5 <sup>a</sup>
Grade 3	1	-	-	-
Inflammation; pigmented macrophages, capsule, focally extensive (note: with intracellular foreign material, hemosiderophages and multinucleated cells)				
Grade 2	-	1	-	-
Atypical proliferation; epithelial, subcapsular, focal				
Grade 2	-	1	-	-

<sup>a</sup>Animal BQ652 was necropsied at day 103 due to procedural-related complications.